

Learning Temporally Extended Skills in Continuous Domains as Symbolic Actions for Planning

Jan Achterhold Markus Krimmel Joerg Stueckler

Embodied Vision Group, Max Planck Institute for Intelligent Systems, Tübingen, Germany

{jan.achterhold,markus.krimmel,joerg.stueckler}@tuebingen.mpg.de

Abstract: Problems which require both long-horizon planning and continuous control capabilities pose significant challenges to existing reinforcement learning agents. In this paper we introduce a novel hierarchical reinforcement learning agent which links temporally extended skills for continuous control with a forward model in a symbolic discrete abstraction of the environment’s state for planning. We term our agent SEADS for Symbolic Effect-Aware Diverse Skills. We formulate an objective and corresponding algorithm which leads to unsupervised learning of a diverse set of skills through intrinsic motivation given a known state abstraction. The skills are jointly learned with the symbolic forward model which captures the effect of skill execution in the state abstraction. After training, we can leverage the skills as symbolic actions using the forward model for long-horizon planning and subsequently execute the plan using the learned continuous-action control skills. The proposed algorithm learns skills and forward models that can be used to solve complex tasks which require both continuous control and long-horizon planning capabilities with high success rate. It compares favorably with other flat and hierarchical reinforcement learning baseline agents and is successfully demonstrated with a real robot. Project page: <https://seads.is.tue.mpg.de>

Keywords: temporally extended skill learning, hierarchical reinforcement learning, diverse skill learning

1 Introduction

Reinforcement learning (RL) agents have been applied to difficult continuous control and discrete planning problems such as the DeepMind Control Suite [1], StarCraft II [2], or Go [3] in recent years. Despite this tremendous success, tasks which require both continuous control capabilities and long-horizon discrete planning are classically approached with task and motion planning [4]. These problems still pose significant challenges to RL agents [5]. An exemplary class of environments which require both continuous-action control and long-horizon planning are *physically embedded games* as introduced by [5]. In these environments, a board game is embedded into a physical manipulation setting. A move in the board game can only be executed indirectly through controlling a physical manipulator such as a robotic arm. We simplify the setting of [5] and introduce physically embedded *single-player* board games which do not require to model the effect of an opponent. Our experiments support the findings of [5] that these environments are challenging to solve for existing flat and hierarchical RL agents. In this paper, we propose a novel hierarchical RL agent for such environments which learns skills and their effects in a known symbolic abstraction of the environment.

As a concrete example for a proposed embedded single-player board game we refer to the *Lights-OutJaco* environment (see Fig. 1). Pushing a field on the *LightsOut* board toggles the illumination state (*on* or *off*) of the field and its non-diagonal neighboring fields. A field on the board can only be pushed by the end effector of the *Jaco* robotic arm. The goal is to reach a board state in which all fields are *off*. The above example also showcases the two concepts of *state* and *action* abstraction in decision making [6]. A state abstraction function $\Phi(s_t)$ only retains information in state s_t which is relevant for a particular decision making task. In the *LightsOut* example, to decide which move to perform next (i.e., which field to push), only the illumination state of the board is relevant. A

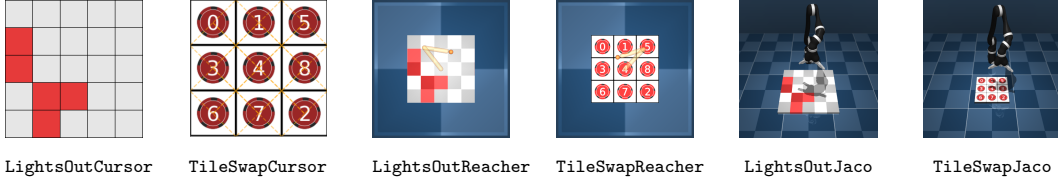


Figure 1: *LightsOut* (with on (red) and off (gray) fields) and *TileSwap* (fields in a rhombus are swapped if pushed inside) board games embedded into physical manipulation settings. A move in the board game can only indirectly be executed through controlling a manipulator.

move can be considered an *action abstraction*: A skill, i.e. high-level action (e.g., push top-left field), comprises a sequence of low-level actions required to control the robotic manipulator.

We introduce a two-layer hierarchical agent which assumes a discrete state abstraction $z_t = \Phi(s_t) \in \mathcal{Z}$ to be known and observable in the environment, which we in the following refer to as *symbolic observation*. In our approach, we assume that state abstractions can be defined manually for the environment. For *LightsOut*, the symbolic observation corresponds to the state of each field (on/off). We provide the state abstraction as prior knowledge about the environment and assume that skills induce changes of the abstract state. Our approach then learns a diverse set of skills for the given state abstraction as action abstractions and a corresponding forward model which predicts the effects of skills on abstract states. In board games, these abstract actions relate to *moves*. We jointly learn the predictive forward model q_θ and *skill policies* $\pi(a | s_t, k)$ for low-level control through an objective which maximizes the number of symbolic states reachable from any state of the environment (diversity) and the predictability of the effect of skill execution. Please see Fig. 2 for an illustration of the introduced temporal and symbolic hierarchy. The forward model q_θ can be leveraged to plan a sequence of skills to reach a particular state of the board (e.g., all fields off), i.e. to solve tasks. We evaluate our approach using two single-player board games in environments with varying complexity in continuous control. We demonstrate that our agent learns skill policies and forward models suitable for solving the associated tasks with high success rate and compares favorably with other flat and hierarchical RL baseline agents. We also demonstrate our agent playing *LightsOut* with a real robot.

In summary, we contribute the following: (1) We formulate a novel RL algorithm which, based on a state abstraction of the environment and an information-theoretic objective, jointly learns a diverse set of continuous-action skills and a forward model capturing the temporally abstracted effect of skill execution in symbolic states. (2) We demonstrate the superiority of our approach compared to other flat and hierarchical baseline agents in solving complex physically-embedded single-player games, requiring high-level planning and continuous control capabilities. We provide additional materials, including video and code, at <https://seads.is.tue.mpg.de>.

2 Related work

Diverse skill learning and skill discovery. Discovering general skills to control the environment through exploration without task-specific supervision is a fundamental challenge in RL research. DIAYN [7] formulates skill discovery using an information-theoretic objective as reward. The agent learns a skill-conditioned policy for which it receives reward if the target states can be well predicted from the skill. VALOR [8] proposes to condition the skill prediction model on the complete trajectory of visited states. Warde-Farley et al. [9] train a goal-conditioned policy to reach diverse states in the environment. Variational Intrinsic Control [10] proposes to use an information-theoretic objective to learn a set of skills which can be identified from their initial and target states. Relative Variational Intrinsic Control [11] seeks to learn skills relative to their start state, aiming to avoid skill representations that merely tile the state space into goal state regions. Both approaches do not learn a forward model on the effect of skill execution like our approach. Sharma et al. [12] propose a model-based RL approach (DADS) which learns a set of diverse skills and their dynamics models using mutual-information-based exploration. While DADS learns skill dynamics as immediate behavior $q(s_{t+1}|s_t, k)$, we learn a transition model on the effect of skills $q(z_T|z_0, k)$ in a symbolic abstraction, thereby featuring temporal abstraction.

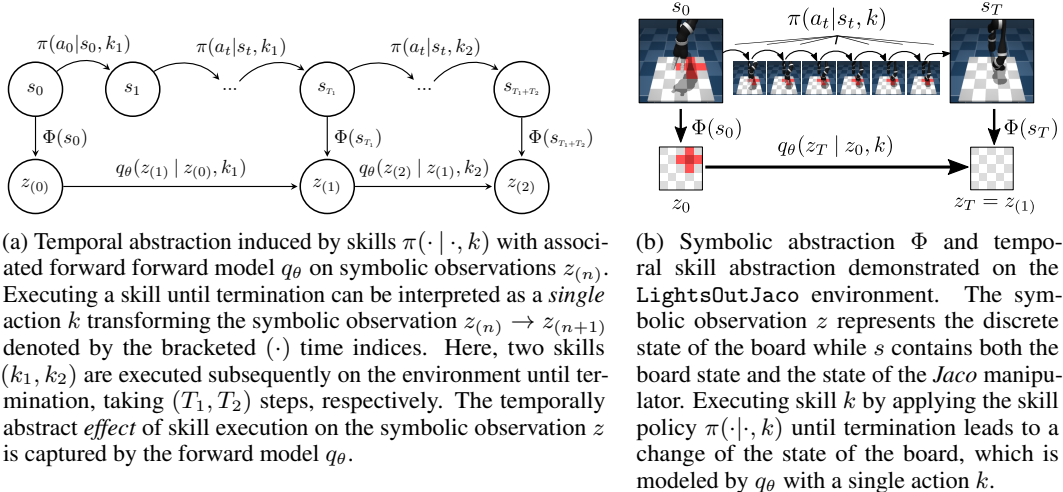


Figure 2: We aim to learn skills with associated policies $\pi(a_t | s_t, k)$ which lead to diverse and predictable (by the forward model q_θ) transitions in a symbolic abstraction $z = \Phi(s)$ of the state s .

Hierarchical RL. Hierarchical RL can overcome sparse reward settings and time extended tasks by breaking the task down into subtasks. Some approaches such as methods based on MAXQ [13, 14] assume prior knowledge on the task-subtask decomposition. In SAC-X [15], auxiliary tasks assist the agent in learning sparse reward tasks and hierarchical learning involves choosing between tasks. Florensa et al. [16] propose to learn a span of skills using stochastic neural networks for representing policies. The policies are trained in a task-agnostic way using a measure of skill diversity based on mutual information. Specific tasks are then tackled by training an RL agent based on the discovered skills. Feudal approaches [17] such as HIRO [18] and HAC [19] train a high-level policy to provide subgoals for a low-level policy. In our method, we impose that a discrete state-action representation exists in which learned skills are discrete actions, and train the discrete forward model and the continuous skill policies jointly. Several approaches to hierarchical RL are based on the options framework [20] which learns policies for temporally extended actions in a two-layer hierarchy. Learning in the options framework is usually driven by task rewards. Recent works extend the framework to continuous spaces and discovery of options (e.g. [21, 22]). HiPPO [23] develop an approximate policy gradient method for hierarchies of actions. HIDIO [24] learns task-agnostic options using a measure of diversity of the skills. In our approach, we also learn task-agnostic (for the given state abstraction) hierarchical representations using a measure of intrinsic motivation. However, an important difference is that we do not learn high-level policies over options using task rewards, but learn a skill-conditional forward model suitable for planning to reach a symbolic goal state. Jointly, continuous policies are learned which implement the skills. Several approaches combine symbolic planning in a given domain description (state and action abstractions) with RL to execute the symbolic actions [25, 26, 27, 28, 29]. Similar to our approach, the work in Guan et al. [29] learns low-level skill policies using an information-theoretic diversity measure which implement known symbolic actions. Differently, we learn the action abstraction and low-level skills given the state abstraction.

Representation learning for symbolic planning. Some research has been devoted to learning representations for symbolic planning. Konidaris et al. [30] propose a method for acquiring a symbolic planning domain from a set of low-level options which implement abstract symbolic actions. In [31] the approach is extended to learning symbolic representations for families of SMDPs which describe options in a variety of tasks. Our approach learns action abstractions as a set of diverse skills given a known state abstraction and a termination condition which requires abstract actions to change abstract states. Toro Icarte et al. [32] learn structure and transition models of finite state machines through RL. Ugur and Piater [33] acquire symbolic forward models for a predefined low-level action repertoire in a robotic manipulation context. Chitnis et al. [34] concurrently learn transition models on the symbolic and low levels from demonstrations provided in the form of hand-designed policies, and use the learned models for bilevel task and motion planning. The approach also assumes the state abstraction function to be known. In [35] a different setting is considered in which the symbolic transition model is additionally assumed known and skill policies that execute symbolic actions

are learned from demonstrations. Other approaches such as DeepSym [36] or LatPlan [37] learn mappings of images to symbolic states and learn action-conditional forward models. In [37] symbolic state-action representations are learned from image observations of discrete abstract actions (e.g. moving puzzle tiles to discrete locations) which already encode the planning problem. Our approach concurrently learns a diverse set of skills (discrete actions) based on an information-theoretic intrinsic reward and the symbolic forward model. Differently, in our approach low-level actions are continuous.

3 Method

Our goal is to learn a hierarchical RL agent which (i) enables high-level, temporally abstract planning to reach a particular goal configuration of the environment (as given by a symbolic observation) and (ii) features continuous control policies to execute the high-level plan. Let \mathcal{S}, \mathcal{A} denote the state and action space of an environment, respectively. In general, by $\mathcal{Z} = \{0, 1\}^D$ we denote the space of discrete symbolic environment observations $z \in \mathcal{Z}$ and assume the existence of a state abstraction $\Phi : \mathcal{S} \rightarrow \mathcal{Z}$. The dimensionality of the symbolic observation D is environment-dependent. For the *LightsOutJaco* environment, the state $s = [q, \dot{q}, z] \in \mathcal{S}$ contains the robot arms’ joint positions and velocities (q, \dot{q}) and a binary representation of the board $z \in \{0, 1\}^{5 \times 5}$. The action space \mathcal{A} is equivalent to the action space of the robotic manipulator. In the *LightsOutJaco* example, it contains the target velocity of all actuatable joints. The discrete variable $k \in \mathcal{K} = \{1, \dots, K\}$ refers to a particular *skill*, which we will detail in the following. The number of skills K needs to be set in advance, but can be chosen larger than the number of actual skills.

We equip our agent with symbolic planning and plan execution capabilities through two components: First, a forward model $\hat{z} = f(z, k) = \operatorname{argmax}_{z'} q_\theta(z' | z, k)$ allows to *enumerate* all possible symbolic successor states \hat{z} of the current symbolic state z by iterating over the discrete variable k . This allows for node expansion in symbolic planners. Second, a family of discretely indexed policies $\pi : \mathcal{A} \times \mathcal{S} \times \mathcal{K} \rightarrow \mathbb{R}$, $a_t \sim \pi(a_t | s_t, k)$ aims to steer the environment into a target state s_T for which it holds that $\Phi(s_T) = \hat{z}$, given that $\Phi(s_0) = z$ and $\hat{z} = \operatorname{argmax}_{z'} q_\theta(z' | z, k)$ (see Fig. 2). We can relate this discretely indexed family of policies to a set of K *options* [20]. An option is formally defined as a triple $o_k = (I_k, \beta_k, \pi_k)$ where $I_k \subseteq \mathcal{S}$ is the set of states in which option k is applicable, $\beta_k : \mathcal{S} \times \mathcal{S} \rightarrow [0, 1]$, $\beta_k(s_0, s_t)$ parametrizes a Bernoulli probability of termination in state s_t when starting in s_0 (f.e. when detecting an abstract state change) and $\pi_k(a | s_t) : \mathcal{S} \rightarrow \Delta(\mathcal{A})$ is the option policy on the action space \mathcal{A} . We will refer to the option policy as *skill policy* in the following. We assume that all options are applicable in all states, i.e., $I_k = \mathcal{S}$. An option terminates if the symbolic state has changed between s_0 and s_t or a timeout is reached, i.e., $\beta_k(s_0, s_t) = \mathbf{1}[\Phi(s_0) \neq \Phi(s_t) \vee t = t_{\max}]$. To this end, we append a normalized counter t/t_{\max} to the state s_t . We define the operator *apply* as $s_T = \operatorname{apply}(E, \pi, s_0, k)$ which applies the skill policy $\pi(a_t | s_t, k)$ until termination on environment E starting from initial state s_0 and returns the terminal state s_T . We also introduce a bracketed time notation which abstracts the effect of skill execution from the number of steps T taken until termination $s_{(n)} = \operatorname{apply}(E, \pi, s_{(n-1)}, k)$ with $n \in \mathbb{N}_0$ (see Fig. 2a). The *apply* operator can thus be rewritten as $s_{(1)} = \operatorname{apply}(E, \pi, s_{(0)}, k)$ with $s_{(0)} = s_0$, $s_{(1)} = s_T$. The symbolic forward model $q_\theta(z_T | z_0, k)$ aims to capture the relation of z_0, k and z_T for $s_T = \operatorname{apply}(E, \pi, s_0, k)$ with $z_0 = \Phi(s_0)$, $z_T = \Phi(s_T)$. The model factorizes over the symbolic observation as $q_\theta(z_T | k, z_0) = \prod_{d=1}^D q_\theta([z_T]_d | k, z_0) = \prod_{d=1}^D \operatorname{Bernoulli}([\alpha_T]_d)$. The Bernoulli probabilities $\alpha_T : \mathcal{Z} \times \mathcal{K} \rightarrow (0, 1)^D$ are predicted by a neural component. We use a multilayer perceptron (MLP) f_θ which predicts the probability p_{flip} of binary variables in z_0 to toggle $p_{\text{flip}} = f_\theta(z_0, k)$. The index operator $[x]_d$ returns the d^{th} element of vector x .

Objective For any state $s_0 \in \mathcal{S}$ with associated symbolic state $z_0 = \Phi(s_0)$ we aim to learn K skills $\pi(a | s_t, k)$ which maximize the diversity in the set of reachable successor states $\{z_T^k = \Phi(\operatorname{apply}(E, \pi, s_0, k)) | k \in \mathcal{K}\}$. Jointly, we aim to model the effect of skill execution with the forward model $q_\theta(z_T | z_0, k)$. Inspired by Variational Intrinsic Control [10] we take an information-theoretic perspective and maximize the mutual information $\mathcal{I}(z_T, k | z_0)$ between the skill index k and the symbolic observation z_T at skill termination given the symbolic observation z_0 at skill initiation, i.e., $\max \mathcal{I}(z_T, k | z_0) = \max H(z_T | z_0) - H(z_T | z_0, k)$. The intuition behind this objective function is that we encourage the agent to (i) reach a diverse set of terminal observations z_T from an initial observation z_0 (by maximizing the conditional entropy $H(z_T | z_0)$) and (ii) behave predictably such that the terminal observation z_T is ideally fully determined by the initial observation z_0 and skill

index k (by minimizing $H(z_T | z_0, k)$). We reformulate the objective as an expectation over tuples (s_0, k, s_T) by employing the mapping function Φ as $\mathcal{I}(z_T, k | z_0) = \mathbb{E}_{(s_0, k, s_T) \sim P} \left[\log \frac{p(z_T | z_0, k)}{p(z_T | z_0)} \right]$ with $z_T := \Phi(s_T)$, $z_0 := \Phi(s_0)$ and replay buffer P . Similar to [12] we derive a lower bound on the mutual information, which is maximized through the interplay of a RL problem and maximum likelihood estimation. To this end, we first introduce a variational approximation $q_\theta(z_T | z_0, k)$ to the transition probability $p(z_T | z_0, k)$, which we model by a neural component. We decompose

$$\mathcal{I}(z_T, k | z_0) = \mathbb{E}_{(s_0, k, s_T) \sim P} \left[\log \frac{q_\theta(z_T | z_0, k)}{p(z_T | z_0)} \right] + \underbrace{\mathbb{E}_{(s_0, k, s_T) \sim P} \left[\log \frac{p(z_T | z_0, k)}{q_\theta(z_T | z_0, k)} \right]}_{\approx \text{D}_{\text{KL}}(p(z_T | z_0, k) || q_\theta(z_T | z_0, k))}$$

giving rise to the lower bound $\mathcal{I}(z_T, k | z_0) \geq \mathbb{E}_{(s_0, k, s_T) \sim P} \left[\log \frac{q_\theta(z_T | z_0, k)}{p(z_T | z_0)} \right]$ whose maximization can be interpreted as a sparse-reward RL problem with reward $\hat{R}_T(k) = \log \frac{q_\theta(z_T | z_0, k)}{p(z_T | z_0)}$. We approximate $p(z_T | z_0)$ as $p(z_T | z_0) \approx \sum_{k'} q_\theta(z_T | z_0, k') p(k' | z_0)$ and assume k uniformly distributed and independent of z_0 , i.e. $p(k' | z_0) = \frac{1}{K}$. This yields a tractable reward

$$R_T(k) = \log \frac{q_\theta(z_T | z_0, k)}{\sum_{k'} q_\theta(z_T | z_0, k')} + \log K. \quad (1)$$

In Sec. 3 we describe modifications we apply to the intrinsic reward R_T which improve the performance of our proposed algorithm. To tighten the lower bound, the KL divergence term in eq. (1) has to be minimized. Minimizing the KL divergence term corresponds to “training” the symbolic forward model q_θ by maximum likelihood estimation of the parameters θ .

Training procedure In each epoch of training, we first collect skill trajectories on the environment using the skill policy π . For each episode $i \in \{1, \dots, N\}$ we reset the environment and obtain an initial state s_0^i . Next, we uniformly sample skills $k^i \sim \text{Uniform}\{1, \dots, K\}$. By iteratively applying the skill policy $\pi(\cdot | \cdot, k^i)$ we obtain resulting states $s_0^i \dots s_{T_i}^i$ and actions $a_0^i \dots a_{T_i-1}^i$. A skill rollout terminates either if an environment-dependent step-limit is reached or when a change in the symbolic observation $z_t \neq z_0$ is observed. We append the rollouts to a limited-size buffer \mathcal{B} . In each training epoch we sample two sets of episodes $\mathcal{S}_{\text{RL}}, \mathcal{S}_{\text{FM}}$ from the buffer for training the policy π and symbolic forward model q_θ . Both episode sets are relabelled as described in Sec. 3. Let $i \in \{1, \dots, M\}$ now refer to the episode index in the set \mathcal{S}_{RL} . From \mathcal{S}_{RL} we sample transition tuples $([s_t^i, k^i], [s_{t+1}^i, k^i], a_t^i, r_{t+1}^i(k^i))$ which are used to update the policy π using the soft actor-critic (SAC) algorithm [38]. To condition the policy on skill k we concatenate k to the state s as denoted by $[\cdot, \cdot]$. We set the intrinsic reward to zero $r_{t+1}^i = 0$ except for the last transition in an episode ($t+1 = T_i$) in which $r_{t+1}^i(k^i) = R(k^i)$. From the episodes in \mathcal{S}_{FM} we form tuples $(z_0^i = \Phi(s_0^i), k^i, z_{T_i}^i = \Phi(s_{T_i}^i))$ which are used to train the symbolic forward model using gradient descent.

Relabelling Early in training, the symbolic transitions caused by skill executions mismatch the predictions of the symbolic forward model. We can in *hindsight* increase the match between skill transitions and forward model by replacing the actual k^i which was used to collect the episode i by a different k_*^i in all transition tuples $([s_t^i, k_*^i], [s_{t+1}^i, k_*^i], a_t^i, r_{t+1}^i(k_*^i))$ and $(z_0^i, k_*^i, z_{T_i}^i)$ of episode i . In particular, we aim to replace k^i by k_*^i which has highest probability $k_*^i = \max_k q_\theta(k | z_T, z_0)$. However, this may lead to an unbalanced distribution over k_*^i after relabelling which is no longer uniform. To this end, we introduce a constrained relabelling scheme as follows. We consider a set of episodes indexed by $i \in \{1, \dots, N\}$ and compute skill log-probabilities for each episode which we denote by $Q_k^i = \log q_\theta(k | z_0^i, z_{T_i}^i)$ where $q_\theta(k | z_0^i, z_{T_i}^i) = \frac{q_\theta(z_{T_i}^i | z_0^i, k)}{\sum_{k'} q_\theta(z_{T_i}^i | z_0^i, k')}$. We find a relabeled skill for each episode (k_*^1, \dots, k_*^N) which maximizes the scoring $\max_{(k_*^1, \dots, k_*^N)} \sum_i Q_{k_*^i}^i$ under the constraint that the counts of re-assigned skills (k_*^1, \dots, k_*^N) and original skills (k^1, \dots, k^N) match, i.e. $\#_{i=1}^N [k_*^i = k] = \#_{i=1}^N [k^i = k] \quad \forall k \in \{1, \dots, K\}$ which is to ensure that after relabelling no skill is over- or underrepresented. The count operator $\#[\cdot]$ counts the number of positive (true) evaluations of its argument in square brackets. This problem can be formulated as a linear sum assignment problem which we solve using the Hungarian method [39, 40]. While we pass all episodes in \mathcal{S}_{FM} to the relabelling module, only a subset (50%) of episodes in \mathcal{S}_{RL} can potentially be relabeled to retain negative examples for the SAC agent. Relabelling experience in hindsight to improve sample efficiency is a common approach in goal-conditioned [41] and hierarchical [19] RL.

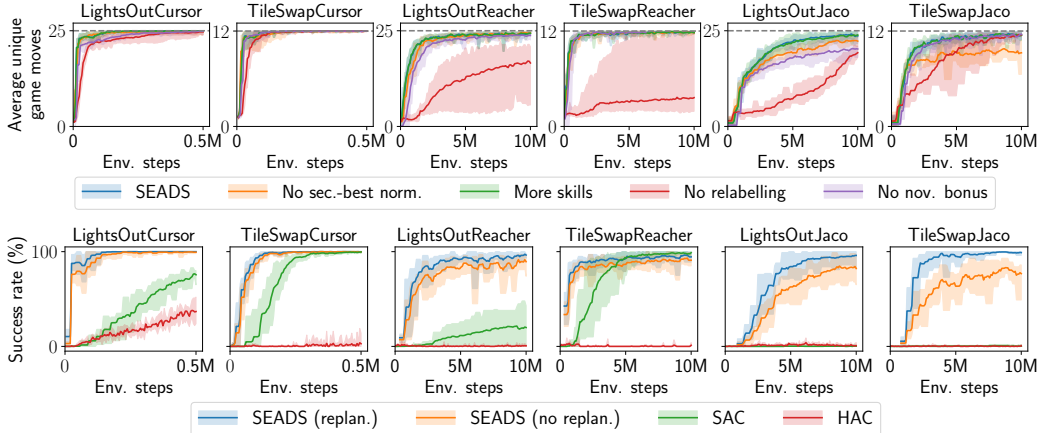


Figure 3: Top row: Number of learned unique game moves for ablations of SEADS. Bottom row: Success rate of the proposed SEADS agent and baseline methods on *LightsOut*, *TileSwap* games embedded in *Cursor*, *Reacher*, *Jaco* environments. SEADS performs comparably or outperforms the baselines on all tasks. The solid line depicts the mean, shaded area min. and max. of 10 (SEADS, SAC on *Cursor*) / 5 (HAC, SAC on *Reacher*, *Jaco*) independently trained agents.

Reward improvements The reward in eq. (1) can be denoted as $R(k) = \log q_\theta(k | z_0, z_T) + \log K$. For numerical stability, we define a lower bounded term $\bar{Q}_k = \text{clip}(\log q_\theta(k | z_0, z_T), \min = -2 \log(K))$ and write $R^0(k) = \bar{Q}_k + \log K$. In our experiments, we observed that occasionally the agent is stuck in a local minimum in which (i) the learned skills are not unique, i.e., two or more skills $k \in \mathcal{K}$ cause the same symbolic transition $z_0 \rightarrow z_T$. In addition, (ii), occasionally, not all possible symbolic transitions are discovered by the agent. To tackle (i) we reinforce the policy π with a positive reward if and only if no other skill k' better fits the symbolic transition ($z_0 \rightarrow z_T$) generated by $\text{apply}(E, \pi, s_0, k)$, i.e., $R^{\text{norm}}(k) = \bar{Q}_k - \text{top2}_{k'} \bar{Q}_{k'}$. which we call **second-best normalization**. The operator $\text{top2}_{k'}$ selects the second-highest value of its argument for $k' \in \mathcal{K}$. We define $R^{\text{base}}(k) = R^{\text{norm}}(k)$ except for the “No second-best norm.” ablation where $R^{\text{base}}(k) = R^0(k)$. To improve (ii) the agent obtains a **novelty bonus** for transitions ($z_0 \rightarrow z_T$) which are not modeled by the symbolic forward model for *any* k' by $R(k) = R^{\text{base}}(k) - \max_{k'} \log q_\theta(z_T | z_0, k')$. If the symbolic state does not change ($z_T = z_0$), we set $R(k) = -2 \log(K)$ (minimal attainable reward).

Planning and skill execution A task is presented to our agent as an initial state of the environment s_0 with associated symbolic observation z_0 and a symbolic goal z^* . First, we leverage our learned symbolic forward model q_θ to plan a sequence of skills k_1, \dots, k_N from z_0 to z^* using breadth-first search (BFS). We use the mode of the distribution over z' for node expansion in BFS: $\text{successor}_{q_\theta}(z, k) = \text{argmax}_{z' \in \mathcal{Z}} q_\theta(z' | z, k)$. After planning, the sequence of skills $[k_1, \dots, k_N]$ is iteratively applied to the environment through $s_{(n)} = \text{apply}(E, \pi, s_{(n-1)}, k_n)$. Inaccuracies of skill execution (leading to different symbolic observations than predicted) can be coped with by replanning after each skill execution. Both single-outcome (mode) determinisation and replanning are common approaches to probabilistic planning [42]. We provide further details in the supplementary material.

4 Experiments

We evaluate our proposed agent on a set of physically-embedded game environments. We follow ideas from [5] but consider single-player games which in principle enable full control over the environment without the existence of an opponent. We chose *LightsOut* and *TileSwap* as board games which are embedded in a physical manipulation scenario with *Cursor*, *Reacher* or *Jaco* manipulators (see Fig. 1). The *LightsOut* game (see Figure 1) consists of a 5×5 board of fields. Each field has a binary illumination state of *on* or *off*. By pushing a field, its illumination state and the state of the (non-diagonally) adjacent fields toggles. At the beginning of the game, the player is presented a board where some fields are on and the others are off. The task of the player is to determine a set of fields to push to obtain a board where all fields are off. The symbolic observation in all *LightsOut* environments represents the illumination state of all 25 fields on the board $\mathcal{Z} = \{0, 1\}^{5 \times 5}$.

In *TileSwap* (see Fig. 1) a 3×3 board is covered by chips numbered from 0 to 8 (each field contains exactly one chip). Initially, the chips are randomly assigned to fields. Two chips can be swapped if they are placed on (non-diagonally) adjacent fields. The game is successfully finished after a number of swap operations if the chips are placed on the board in ascending order. In all *TileSwap* environments the symbolic observation represents whether the i -th chip is located on the j -th field $\mathcal{Z} = \{0, 1\}^{9 \times 9}$. To ensure feasibility, we apply a number of random moves (pushes/swaps) to the goal board configuration of the respective game. We quantify the difficulty of a particular board configuration by the number of moves required to solve the game. We ensure disjointness of board configurations used for training and testing through a hashing algorithm (see supp. material). A board game move (“push” in *LightsOut*, “swap” in *TileSwap*) is triggered by the manipulator’s end effector touching a particular position on the board. We use three manipulators of different complexity (see Fig. 1). The *Cursor* manipulator can be navigated on the 2D game board by commanding x and y displacements. The board coordinates are $x, y \in [0, 1]$, the maximum displacement per timestep is $\Delta x, \Delta y = 0.2$. A third action triggers a push (*LightsOut*) or swap (*TileSwap*) at the current position of the cursor. The *Reacher* [1] manipulator consists of a two-link arm with two rotary joints. The position of the end effector in the 2D plane can be controlled by external torques applied to the two rotary joints. As for the *Cursor* manipulator an additional action triggers a game move at the current end effector coordinates. The *Jaco* manipulator [43] is a 9-DoF robotic arm whose joints are velocity-controlled at 10Hz. It has an end-effector with three “fingers” which can touch the underlying board to trigger game moves. The arm is reset to a random configuration above the board around the board’s center after a game move (details in supplementary material). By combining the games of *LightsOut* and *TileSwap* with the *Cursor*, *Reacher* and *Jaco* manipulators we obtain six environments. For the step limit for skill execution we set 10 steps on *Cursor* and 50 steps in *Reacher* and *Jaco* environments. With our experiments we aim at answering the following research questions: **R1**: How many distinct skills are learned by SEADS? Does SEADS learn all 25 (12) possible moves in *LightsOut* (*TileSwap*) reliably? **R2**: How do our design choices contribute to the performance of SEADS? **R3**: How well does SEADS perform in solving the posed tasks in comparison to other flat and hierarchical RL approaches? **R4**: Can our SEADS also be trained and applied on a real robot?

Skill learning evaluation To address **R1** we investigate how many distinct skills are learned by SEADS. If not all possible moves within the board games are learned as skills (25 for *LightsOut*, 12 for *TileSwap*), some initial configurations can become unsolvable for the agent, negatively impacting task performance. To count the number of learned skills we apply each skill $k \in \{1, \dots, K\}$ on a fixed initial state s_0 of the environment E until termination (i.e., $\text{apply}(E, s_0, \pi, k)$). Among these K skill executions we count the number of unique game moves being triggered. We report the average number of unique game moves for $N = 100$ distinct initial states s_0 . On the *Cursor* environments SEADS detects nearly all possible game moves (avg. approx. 24.9 of 25 possible in *LightsOutCursor*, 12 of 12 in *TileSwapCursor*). For *Reacher* almost all moves are found (24.3/11.8), while in the *Jaco* environments some moves are missing occasionally (23.6/11.5), for the last checkpoints taken before reaching $5 \cdot 10^5$ (*Cursor*), 10^7 (*Reacher*, *Jaco*) env. steps (see Sec. S.8.1 for details). We demonstrate superior performance compared to a baseline skill discovery method (Variational Intrinsic Control, Gregor et al. [10]) in the supplementary material. We substantiate our agent design decisions through an ablation study (**R2**) in which we compare the number of unique skills (game moves) detected for several variants of SEADS (see Fig. 3). In a first study, we remove single parts from our agent to quantify their impact on performance. This includes training SEADS without the proposed *relabelling*, *second-best normalization* and *novelty bonus*. We found all of these innovations to be important for the performance of SEADS, with the difference to the full SEADS agent being most prominent in the *LightsOutJaco* environment. Learning with *more skills* (15 for *TileSwap*, 30 for *LightsOut*) than actually needed does not harm performance.

Task performance evaluation To evaluate the task performance of our agent and baseline agents (**R3**) we initialize the environments such that the underlying board game requires at maximum 5 moves (pushes in *LightsOut*, swaps in *TileSwap*, limited due to branching factor and BFS) to be solved. We evaluate each agent on 20 examples for each number of moves in $\{1, \dots, 5\}$ required to solve the game. We consider a task to be successfully solved if the target board configuration was reached (all fields *off* in *LightsOut*, ordered field in *TileSwap*). For SEADS we additionally count tasks as “failed” if planning exceeds a wall time limit of 60 seconds. We evaluate both planning variants with and without replanning. As an instance of a flat (non-hierarchical) agent we evaluate the performance of Soft Actor-Critic

(SAC [38]). The SAC agent receives the full environment state $s \in \mathcal{S}$ which includes the symbolic observation (board state). It obtains a reward of 1 if it successfully solved the game and 0 otherwise. In contrast to the Soft Actor-Critic agent the SEADS agent leverages the decomposition of state $s \in \mathcal{S}$ and symbolic observation $z \in \mathcal{Z}$. For a fair comparison to a hierarchical agent, we consider Hierarchical Actor-Critic (HAC, Levy et al. [19]), which, similar to SEADS, can also leverage the decomposition of s and z . We employ a two-level hierarchy in which the high-level policy sets *symbolic* subgoals $z \in \mathcal{Z}$ to the low-level policy, thereby leveraging the access to the symbolic observation. We refer to the supplementary material for implementation and training details of SAC and HAC. Fig. 3 visualizes the performance of SEADS and the baselines. On all environments SEADS performs similar or outperforms the baselines, with the performance difference being most pronounced on the *Jaco* environments on which SAC and HAC do not make any progress. On the *Cursor* environments SEADS achieves a success rate of 100%. On the remaining environments, the average success rate (with replanning) is 95.8% (*LightsOutReacher*), 95.5% (*TileSwapReacher*), 94.9% (*LightsOutJaco*), 98.8% (*TileSwapJaco*). These results are obtained at the last common checkpoints before reaching $5 \cdot 10^5$ (*Cursor*) / 10^7 (*Reacher, Jaco*) env. steps (see Sec. S.8.1 for details).

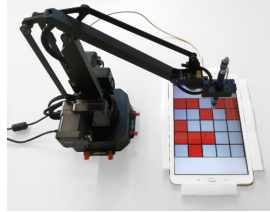


Figure 4: Robot setup.

Robot experiment To evaluate the applicability of our approach on a real-world robotic system (**R4**) we set up a testbed with a uArm Swift Pro robotic arm which interacts with a tablet using a capacitive pen (see Fig. 4). The SEADS agent commands a displacement $|\Delta x|, |\Delta y| \leq 0.2$ and an optional pushing command as in the *Cursor* environments. The board state is communicated to the agent through the tablet’s USB interface. We manually reset the board *once* at the beginning of training, and do not interfere in the further process. After training for $\approx 160k$ interactions (≈ 43.5 hours) the agent successfully solves all boards in a test set of 25 board configurations (5 per solution depth in $\{1, \dots, 5\}$). We refer to the supplementary material for details and a video.

5 Assumptions and Limitations

Our approach assumes that the state abstraction is known, the symbolic observation z is provided by the environment, and that the continuous state is fully observable. Learning the state abstraction too is an interesting direction for future research. The breadth-first search planner we use for planning on the symbolic level exhibits scaling issues for large solution depths; e.g., for *LightsOut* it exceeds a 5-minute threshold for solution depths (number of initial board perturbations) ≥ 9 . In future work, more efficient heuristic or probabilistic planners could be explored. Currently, our BFS planner produces plans which are optimal with respect to the number of skills executed. Means for predicting and taking the skill execution cost into account for planning could be pursued in future work. In the more complex environments (*Reacher, Jaco*) we observe our agent to not learn all possible skills reliably, in particular for skills for which no transitions exist in the replay buffer. In future work one could integrate additional exploration objectives which incentivize to visit unseen regions of the state space. Also, the approach is currently limited to settings such as in board games, where all symbolic state transitions should be mapped to skills. It is an open research question how our skill exploration objective could be combined with demonstrations or task-specific objectives to guide the search for symbolic actions and limit the search space in more complex environments.

6 Conclusion

We present an agent which, in an unsupervised way, learns diverse skills in complex physically embedded board game environments which relate to *moves* in the particular games. We assume a state abstraction from continuous states to symbolic states known and observable to the agent as prior information, and that skills lead to changes in the symbolic state. The jointly learned forward model captures the temporally extended *effects* of skill execution. We leverage this forward model to plan over a sequence of skills (moves) to solve a particular task, i.e., bring the game board to a desired state. We demonstrate that with this formulation we can solve complex physically embedded games with high success rate, that our approach compares favorably with other flat and hierarchical RL algorithms, and also transfers to a real robot. Our approach provides an unsupervised learning alternative to prescribing the action abstraction and pretraining each skill individually before learning a forward model from skill executions. In future research, our approach could be combined with state abstraction learning to leverage its full potential.

Acknowledgments

This work was supported by Max Planck Society and Cyber Valley. The authors thank the International Max Planck Research School for Intelligent Systems (IMPRS-IS) for supporting Jan Achterhold.

References

- [1] Y. Tassa, Y. Doron, A. Muldal, T. Erez, Y. Li, D. de Las Casas, D. Budden, A. Abdolmaleki, J. Merel, A. Lefrancq, T. P. Lillicrap, and M. A. Riedmiller. “DeepMind Control Suite”. In: *CoRR* abs/1801.00690 (2018). arXiv: 1801.00690. URL: <http://arxiv.org/abs/1801.00690>.
- [2] O. Vinyals, I. Babuschkin, W. M. Czarnecki, M. Mathieu, A. Dudzik, J. Chung, D. H. Choi, R. Powell, T. Ewalds, P. Georgiev, J. Oh, D. Horgan, M. Kroiss, I. Danihelka, A. Huang, L. Sifre, T. Cai, J. P. Agapiou, M. Jaderberg, A. S. Vechnyevets, R. Leblond, T. Pohlen, V. Dalibard, D. Budden, Y. Sulsky, J. Molloy, T. L. Paine, Ç. Gülçehre, Z. Wang, T. Pfaff, Y. Wu, R. Ring, D. Yogatama, D. Wünsch, K. McKinney, O. Smith, T. Schaul, T. P. Lillicrap, K. Kavukcuoglu, D. Hassabis, C. Apps, and D. Silver. “Grandmaster level in StarCraft II using multi-agent reinforcement learning”. In: *Nature* 575.7782 (2019), pp. 350–354. DOI: 10.1038/s41586-019-1724-z. URL: <https://doi.org/10.1038/s41586-019-1724-z>.
- [3] D. Silver, A. Huang, C. J. Maddison, A. Guez, L. Sifre, G. van den Driessche, J. Schrittwieser, I. Antonoglou, V. Panneershelvam, M. Lanctot, S. Dieleman, D. Grewe, J. Nham, N. Kalchbrenner, I. Sutskever, T. Lillicrap, M. Leach, K. Kavukcuoglu, T. Graepel, and D. Hassabis. “Mastering the Game of Go with Deep Neural Networks and Tree Search”. In: *Nature* 529.7587 (Jan. 2016), pp. 484–489. DOI: 10.1038/nature16961.
- [4] C. R. Garrett, R. Chitnis, R. Holladay, B. Kim, T. Silver, L. P. Kaelbling, and T. Lozano-Pérez. “Integrated Task and Motion Planning”. In: *Annual Review of Control, Robotics, and Autonomous Systems* 4.1 (2021), pp. 265–293. eprint: <https://doi.org/10.1146/annurev-control-091420-084139>. URL: <https://doi.org/10.1146/annurev-control-091420-084139>.
- [5] M. Mirza, A. Jaegle, J. J. Hunt, A. Guez, S. Tunyasuvunakool, A. Muldal, T. Weber, P. Karkus, S. Racanière, L. Buesing, T. P. Lillicrap, and N. Heess. “Physically Embedded Planning Problems: New Challenges for Reinforcement Learning”. In: *CoRR* abs/2009.05524 (2020). arXiv: 2009.05524. URL: <https://arxiv.org/abs/2009.05524>.
- [6] G. Konidaris. “On the necessity of abstraction”. In: *Current Opinion in Behavioral Sciences* 29 (2019). Artificial Intelligence, pp. 1–7. DOI: <https://doi.org/10.1016/j.cobeha.2018.11.005>.
- [7] B. Eysenbach, A. Gupta, J. Ibarz, and S. Levine. “Diversity is All You Need: Learning Skills without a Reward Function”. In: *7th International Conference on Learning Representations (ICLR)*. 2019. URL: <https://openreview.net/forum?id=SJx63jRqFm>.
- [8] J. Achiam, H. Edwards, D. Amodei, and P. Abbeel. “Variational Option Discovery Algorithms”. In: *CoRR* abs/1807.10299 (2018). arXiv: 1807.10299. URL: <http://arxiv.org/abs/1807.10299>.
- [9] D. Warde-Farley, T. V. de Wiele, T. D. Kulkarni, C. Ionescu, S. Hansen, and V. Mnih. “Unsupervised Control Through Non-Parametric Discriminative Rewards”. In: *7th International Conference on Learning Representations (ICLR)*. 2019. URL: <https://openreview.net/forum?id=r1eVMnA9K7>.
- [10] K. Gregor, D. J. Rezende, and D. Wierstra. “Variational Intrinsic Control”. In: *International Conference on Learning Representations (ICLR), Workshop Track Proceedings*. 2017. URL: <https://openreview.net/forum?id=Skc-Fo4Yg>.
- [11] K. Baumli, D. Warde-Farley, S. Hansen, and V. Mnih. “Relative Variational Intrinsic Control”. In: *AAAI Conference on Artificial Intelligence (AAAI)*. 2021, pp. 6732–6740. URL: <https://ojs.aaai.org/index.php/AAAI/article/view/16832>.
- [12] A. Sharma, S. Gu, S. Levine, V. Kumar, and K. Hausman. “Dynamics-Aware Unsupervised Discovery of Skills”. In: *8th International Conference on Learning Representations (ICLR)*. 2020. URL: <https://openreview.net/forum?id=HJgLZR4KvH>.
- [13] T. G. Dietterich. “Hierarchical Reinforcement Learning with the MAXQ Value Function Decomposition”. In: *J. Artif. Intell. Res.* 13 (2000), pp. 227–303. DOI: 10.1613/jair.639. URL: <https://doi.org/10.1613/jair.639>.

- [14] Z. Li, A. Narayan, and T.-Y. Leong. “An Efficient Approach to Model-Based Hierarchical Reinforcement Learning”. In: *Proceedings of the Thirty-First AAAI Conference on Artificial Intelligence (AAAI)*. 2017, pp. 3583–3589. URL: <http://aaai.org/ocs/index.php/AAAI/AAAI17/paper/view/14771>.
- [15] M. A. Riedmiller, R. Hafner, T. Lampe, M. Neunert, J. Degraeve, T. V. de Wiele, V. Mnih, N. Heess, and J. T. Springenberg. “Learning by Playing Solving Sparse Reward Tasks from Scratch”. In: *Proceedings of the 35th International Conference on Machine Learning (ICML)*. Vol. 80. Proceedings of Machine Learning Research. PMLR, 2018, pp. 4341–4350. URL: <http://proceedings.mlr.press/v80/riedmiller18a.html>.
- [16] C. Florensa, Y. Duan, and P. Abbeel. “Stochastic Neural Networks for Hierarchical Reinforcement Learning”. In: *5th International Conference on Learning Representations (ICLR)*. 2017. URL: <https://openreview.net/forum?id=B1oK8aoxe>.
- [17] P. Dayan and G. E. Hinton. “Feudal Reinforcement Learning”. In: *Advances in Neural Information Processing Systems (NeurIPS)*. Ed. by S. J. Hanson, J. D. Cowan, and C. L. Giles. 1992, pp. 271–278. URL: <http://papers.nips.cc/paper/714-feudal-reinforcement-learning>.
- [18] O. Nachum, S. Gu, H. Lee, and S. Levine. “Data-Efficient Hierarchical Reinforcement Learning”. In: *Advances in Neural Information Processing Systems (NeurIPS)*. 2018, pp. 3307–3317. URL: <https://proceedings.neurips.cc/paper/2018/hash/e6384711491713d29bc63fc5eeb5ba4f-Abstract.html>.
- [19] A. Levy, G. D. Konidaris, R. P. Jr., and K. Saenko. “Learning Multi-Level Hierarchies with Hindsight”. In: *7th International Conference on Learning Representations (ICLR)*. 2019. URL: <https://openreview.net/forum?id=ryzEC0AcY7>.
- [20] R. S. Sutton, D. Precup, and S. P. Singh. “Between MDPs and Semi-MDPs: A Framework for Temporal Abstraction in Reinforcement Learning”. In: *Artif. Intell.* 112.1-2 (1999), pp. 181–211. DOI: 10.1016/S0004-3702(99)00052-1.
- [21] P.-L. Bacon, J. Harb, and D. Precup. “The Option-Critic Architecture”. In: *Proceedings of the Thirty-First AAAI Conference on Artificial Intelligence (AAAI)*. Ed. by S. Singh and S. Markovitch. 2017, pp. 1726–1734. URL: <http://aaai.org/ocs/index.php/AAAI/AAAI17/paper/view/14858>.
- [22] A. Bagaria and G. Konidaris. “Option Discovery using Deep Skill Chaining”. In: *8th International Conference on Learning Representations (ICLR)*. 2020. URL: <https://openreview.net/forum?id=B1gqipNYwH>.
- [23] A. C. Li, C. Florensa, I. Clavera, and P. Abbeel. “Sub-policy Adaptation for Hierarchical Reinforcement Learning”. In: *8th International Conference on Learning Representations (ICLR)*. 2020. URL: <https://openreview.net/forum?id=ByeWogStDS>.
- [24] J. Zhang, H. Yu, and W. Xu. “Hierarchical Reinforcement Learning By Discovering Intrinsic Options”. In: *International Conference on Learning Representations (ICLR)*. 2021.
- [25] M. R. K. Ryan. “Using Abstract Models of Behaviours to Automatically Generate Reinforcement Learning Hierarchies”. In: *International Conference on Machine Learning (ICML)*. 2002, pp. 522–529.
- [26] D. Lyu, F. Yang, B. Liu, and S. Gustafson. “SDRL: Interpretable and Data-Efficient Deep Reinforcement Learning Leveraging Symbolic Planning”. In: *The Thirty-Third AAAI Conference on Artificial Intelligence (AAAI)*. 2019, pp. 2970–2977.
- [27] L. Illanes, X. Yan, R. T. Icarte, and S. A. McIlraith. “Symbolic Plans as High-Level Instructions for Reinforcement Learning”. In: *Proceedings of the Thirtieth International Conference on Automated Planning and Scheduling (ICAPS)*. Ed. by J. C. Beck, O. Buffet, J. Hoffmann, E. Karpas, and S. Sohrabi. AAAI Press, 2020, pp. 540–550.
- [28] H. Kokel, A. Manoharan, S. Natarajan, B. Ravindran, and P. Tadepalli. “RePREL: Integrating Relational Planning and Reinforcement Learning for Effective Abstraction”. In: *Proceedings of the Thirty-First International Conference on Automated Planning and Scheduling (ICAPS)*. 2021, pp. 533–541.
- [29] L. Guan, S. Sreedharan, and S. Kambhampati. “Leveraging Approximate Symbolic Models for Reinforcement Learning via Skill Diversity”. In: *International Conference on Machine Learning (ICML)*. Vol. 162. Proceedings of Machine Learning Research. PMLR, 2022, pp. 7949–7967. URL: <https://proceedings.mlr.press/v162/guan22c.html>.

- [30] G. Konidaris, L. P. Kaelbling, and T. Lozano-Perez. “From Skills to Symbols: Learning Symbolic Representations for Abstract High-Level Planning”. In: *J. Artif. Int. Res.* 61.1 (Jan. 2018), pp. 215–289.
- [31] S. James, B. Rosman, and G. Konidaris. “Learning Portable Representations for High-Level Planning”. In: *Proceedings of the 37th International Conference on Machine Learning*. Vol. 119. Proceedings of Machine Learning Research. PMLR, 13–18 Jul 2020, pp. 4682–4691. URL: <https://proceedings.mlr.press/v119/james20a.html>.
- [32] R. Toro Icarte, E. Waldie, T. Klassen, R. Valenzano, M. Castro, and S. McIlraith. “Learning Reward Machines for Partially Observable Reinforcement Learning”. In: *Advances in Neural Information Processing Systems (NeurIPS)*. Vol. 32. 2019. URL: <https://proceedings.neurips.cc/paper/2019/file/532435c44bec236b471a47a88d63513d-Paper.pdf>.
- [33] E. Ugur and J. Piater. “Bottom-up learning of object categories, action effects and logical rules: From continuous manipulative exploration to symbolic planning”. In: *IEEE International Conference on Robotics and Automation (ICRA)*. 2015, pp. 2627–2633. DOI: 10.1109/ICRA.2015.7139553.
- [34] R. Chitnis, T. Silver, J. B. Tenenbaum, T. Lozano-Perez, and L. P. Kaelbling. “Learning Neuro-Symbolic Relational Transition Models for Bilevel Planning”. In: *IEEE/RSJ Int. Conf. on Intelligent Robots and Systems (IROS)*. 2022.
- [35] T. Silver, A. Athalye, J. B. Tenenbaum, T. Lozano-Perez, and L. P. Kaelbling. “Learning Neuro-Symbolic Skills for Bilevel Planning”. In: *Conference on Robot Learning (CoRL)*. 2022. URL: <https://openreview.net/pdf?id=0IaJRUo5UXy>.
- [36] A. Ahmetoglu, M. Y. Seker, A. Sayin, S. Bugur, J. H. Piater, E. Öztop, and E. Ugur. “DeepSym: Deep Symbol Generation and Rule Learning from Unsupervised Continuous Robot Interaction for Planning”. In: *CoRR* abs/2012.02532 (2020). arXiv: 2012.02532. URL: <https://arxiv.org/abs/2012.02532>.
- [37] M. Asai and A. Fukunaga. “Classical Planning in Deep Latent Space: Bridging the Subsymbolic-Symbolic Boundary”. In: *Proceedings of the Thirty-Second AAAI Conference on Artificial Intelligence (AAAI)*. 2018, pp. 6094–6101. URL: <https://www.aaai.org/ocs/index.php/AAAI/AAAI18/paper/view/16302>.
- [38] T. Haarnoja, A. Zhou, P. Abbeel, and S. Levine. “Soft Actor-Critic: Off-Policy Maximum Entropy Deep Reinforcement Learning with a Stochastic Actor”. In: *Proceedings of the 35th International Conference on Machine Learning (ICML)*. Vol. 80. Proceedings of Machine Learning Research. PMLR, 2018, pp. 1856–1865. URL: <http://proceedings.mlr.press/v80/haarnoja18b.html>.
- [39] H. W. Kuhn. “The Hungarian method for the assignment problem”. In: *Naval research logistics quarterly* 2.1-2 (1955), pp. 83–97.
- [40] J. Munkres. “Algorithms for the assignment and transportation problems”. In: *Journal of the society for industrial and applied mathematics* 5.1 (1957), pp. 32–38.
- [41] M. Andrychowicz, D. Crow, A. Ray, J. Schneider, R. Fong, P. Welinder, B. McGrew, J. Tobin, P. Abbeel, and W. Zaremba. “Hindsight Experience Replay”. In: *Advances in Neural Information Processing Systems (NeurIPS)*. 2017, pp. 5048–5058. URL: <http://papers.nips.cc/paper/7090-hindsight-experience-replay>.
- [42] S. W. Yoon, A. Fern, and R. Givan. “FF-Replan: A Baseline for Probabilistic Planning”. In: *Proceedings of the Seventeenth International Conference on Automated Planning and Scheduling (ICAPS)*. 2007, p. 352. URL: <http://www.aaai.org/Library/ICAPS/2007/icaps07-045.php>.
- [43] A. Campeau-Lecours, H. Lamontagne, S. Latour, P. Fauteux, V. Maheu, F. Boucher, C. Deguire, and L.-J. C. L’Ecuyer. “Kinova Modular Robot Arms for Service Robotics Applications”. In: *Int. J. Robotics Appl. Technol.* 5.2 (2017), pp. 49–71. DOI: 10.4018/IJRAT.2017070104. URL: <https://doi.org/10.4018/IJRAT.2017070104>.

S.1 Introduction

In the following we provide supplementary details and analysis of our approach. We show visualisations of the learned skills in Sec. S.2 and provide an analysis for solution depths > 5 in Sec. S.3. In Sec. S.4 we introduce additional embedded *LightsOut* environments, featuring a 3D board and larger board sizes, to evaluate the exploration capabilities and limitations of our method. In Sec. S.5 we give details on the robot experiment, and provide additional ablation results in Sec. S.6. Architectural and implementation details are given in Sec. S.8 for SEADS, in Sec. S.9 for the SAC baseline and in Sec. S.10 for the HAC baseline. In Sec. S.11 we compare SEADS to a variant which uses a skill discriminator instead of a forward model as in "Variational Intrinsic Control" (VIC, Gregor et al. [1]). In Sec. S.12 we detail how we define training and test splits on our proposed environments. Finally, we present detailed results for hyperparameter search on the SAC and HAC baselines in Sec. S.13.

S.2 Learned skills

We provide additional visualizations on the behaviour of SEADS in Fig. S.5, showing that SEADS learns to assign skills to pushing individual fields on the game boards.

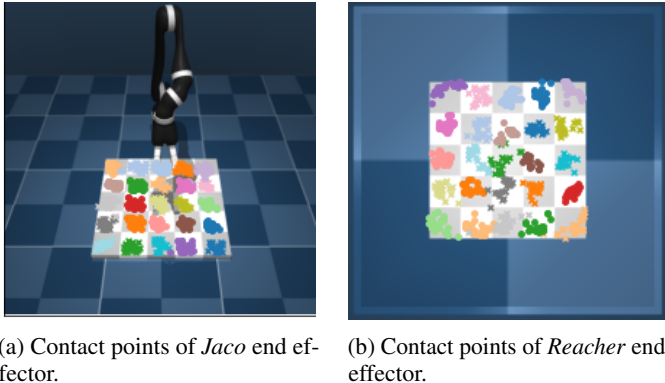


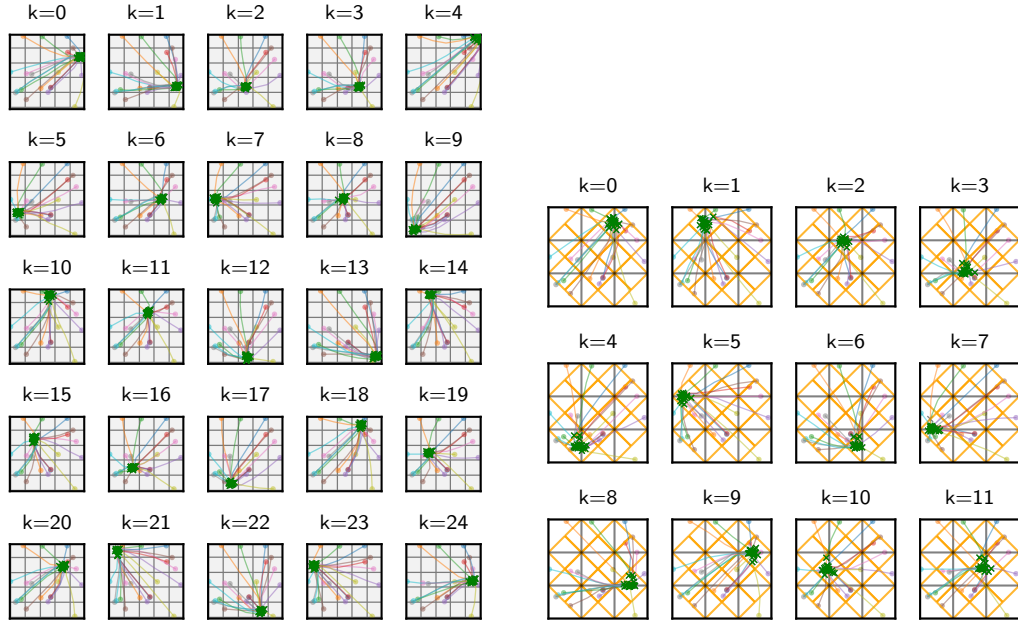
Figure S.5: Contact points of the *Jaco* (*Reacher*) end effector in the *LightsOutCursor* (*LightsOutReacher*) environments when executing skill $k \in \{1, \dots, 25\}$ on 20 different initializations of the environment. Each skill is assigned a unique color/marker combination. We show the agent performance after 1×10^7 environment steps. We observe that the SEADS agent learns to push individual fields as skills.

S.2.1 Skill trajectories

In Figs. S.6, S.7 and S.8 we provide visualizations of trajectories executed by the learned skills on the *Cursor*, *Reacher* and *Jaco* environments.

S.2.2 Solution length

In Fig. S.9 we provide an analysis how many low-level environment steps (i.e., manipulator actions) are executed to solve instances of the presented physically embedded board games. We follow the evaluation procedure of the main paper (Fig. 3) and show results for 10 trained agents and 20 initial board configurations for each solution depth in $\{1, \dots, 5\}$. We only report results on board configurations which are successfully solved by SEADS. We observe that even for a solution depth of 5, for the *Cursor* environments, only relatively few environment steps are required in total to solve the board game (≈ 15 for *LightsOutCursor*, ≈ 10 for *TileSwapCursor*). In contrast, the more complex *Reacher* and *Jaco* environments require significantly more interactions to be solved, with up to 400 steps executed on *TileSwapJaco* for a solution depth of 5 and enabled re-planning.



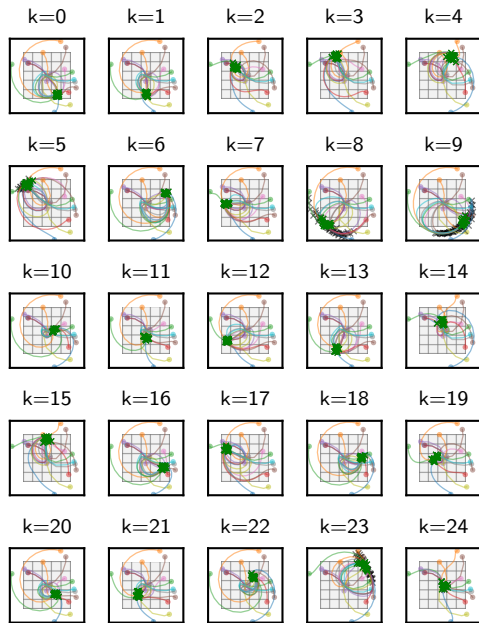
(a) Skill trajectories on LightsOutCursor.

(b) Skill trajectories on TileSwapCursor.

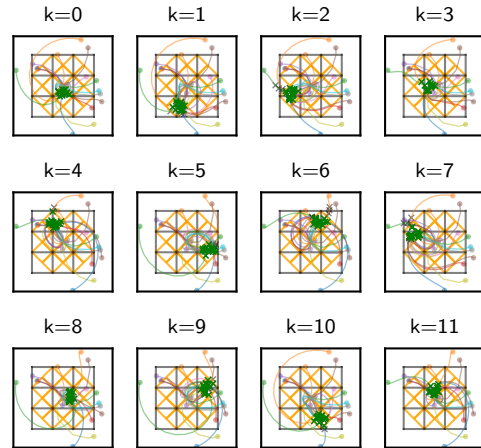
Figure S.6: Trajectories in *Cursor*-embedded environments for skills k on 20 different environment initializations. Colored lines show the x, y -coordinates of the Cursor, with the circular marker indicating the start position of the skill. Black markers indicate locations where a "push" was executed, and green markers where the push has caused a change in the symbolic state.

S.2.3 Skill length

Following the evaluation procedure from Sec. S.2.2 we report the distribution of skill lengths (i.e., number of actions applied to the manipulator per skill) in Fig. S.10. Again, we only include problem instances which were successfully solved by SEADS. While skill executions on the *Cursor* environments are typically short (median 3/2 manipulator actions for LightsOutCursor/TileSwapCursor), the *Reacher* and *Jaco* environments require a higher number of manipulator actions per skill (median 11/12/9/13 for LightsOutReacher/LightsOutJaco/TileSwapReacher/TileSwapJaco).

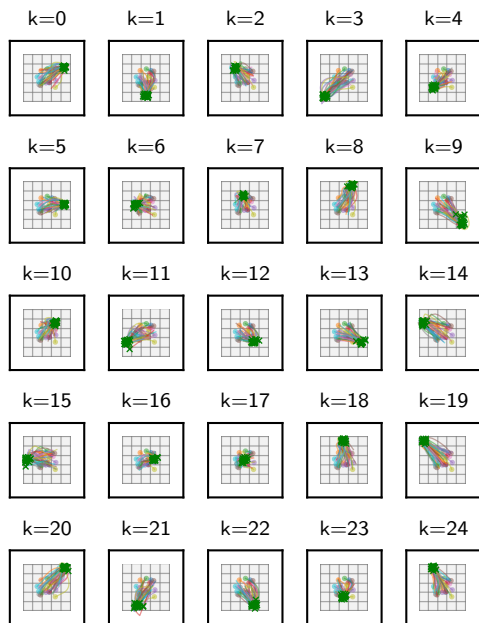


(a) Skill trajectories on `LightsOutReacher`.

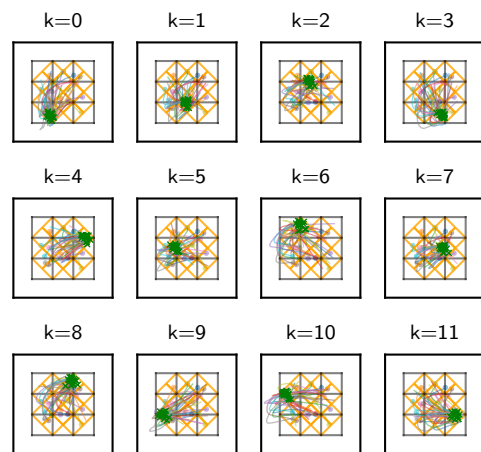


(b) Skill trajectories on `TileSwapReacher`.

Figure S.7: Trajectories in *Reacher*-embedded environments for skills k on 20 different environment initializations. Colored lines show the x, y -coordinates of the Reacher end-effector, with the circular marker indicating the start position of the skill. Black markers indicate locations where a "push" was executed, and green markers where the push has caused a change in the symbolic state.



(a) Skill trajectories on `LightsOutJaco`.



(b) Skill trajectories on `TileSwapJaco`.

Figure S.8: Trajectories in *Jaco*-embedded environments for skills k on 20 different environment initializations. Colored lines show the x, y -coordinates of the Jaco hand, with the circular marker indicating the start position of the skill. Green markers indicate contact locations with the board.

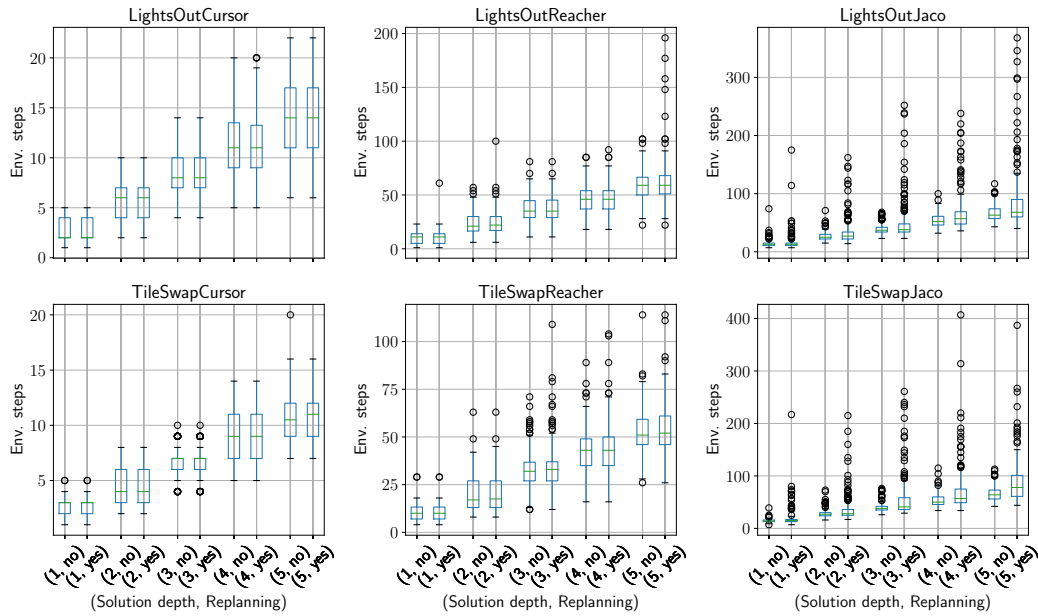


Figure S.9: Analysis of solution lengths (total number of manipulator steps required to solve the physically embedded board games) for different environments, solution depths and planning with/without re-planning. Box-plots show the 25%/75% quartiles and median (green line). Whiskers extend to the farthest datapoint within the 1.5-fold interquartile range. Outliers are plotted as circles.

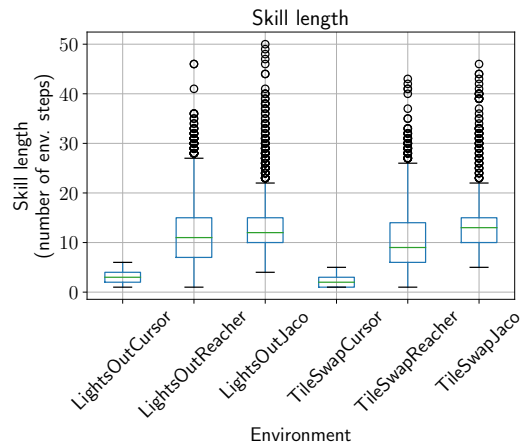


Figure S.10: Analysis of skill lengths (number of manipulator steps executed within a single skill) for different environments. Box-plots show the 25%/75% quartiles and median (green line). Whiskers extend to the farthest datapoint within the 1.5-fold interquartile range. Outliers are plotted as circles.

S.3 Large solution depth analysis

In Fig. S.11 we present an analysis for solving *LightsOut* tasks with solution depths > 5 using the learned SEADS agent on *LightsOutCursor*. We observe a high mean success rate of $\geq 98\%$ for solution depths ≤ 8 . However, the time required for the breadth-first search planner to find a feasible plan increases from $\approx 2.02s$ for solution depth 5 to $\approx 301.8s$ for solution depth 9. We abort BFS planning if the list of nodes to expand exceeds a size of ≈ 16 GB memory usage. All experiments were conducted on Intel® Xeon® Gold 5220 CPUs with a clock rate of 2.20 GHz.

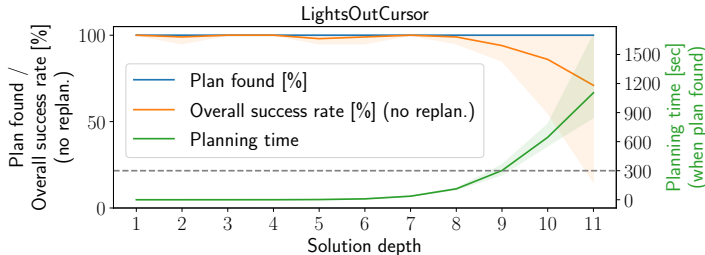


Figure S.11: Analysis of the *LightsOutCursor* environment for solution depths > 5 . "Solution depth" is the number of game moves required to solve the *LightsOut* instance. "Plan found" refers to the ratio of problem instances where BFS finds a feasible plan. "Overall success rate" quantifies the ratio of problem instances for which a feasible plan was found and, in addition, was successfully executed by the low-level policy. The "Planning time" refers to the wall-time the breadth-first search planner runs, for the cases in which it finds a feasible plan. We report results for 20 problem instances for each solution depth for 5 independently trained agents. We refer to sec. S.3 for details. The solid line refers to the mean, shaded area to min/max over 5 independently trained agents.

S.4 Additional LightsOut variants

S.4.1 LightsOut3DJaco

In addition to the *LightsOutJaco* environment presented in the main paper we introduce an additional environment *LightsOut3DJaco*. While in *LightsOutJaco* the *LightsOut* board is a flat plane, in *LightsOut3DJaco* the fields are elevated/recessed depending on their distance to the board's center (see Fig. S.12). This poses an additional challenge to the agent, as it has to avoid to push fields with its fingers accidentally during skill execution. Despite the increased complexity of *LightsOut3DJaco* over *LightsOutJaco* we observe similar results in terms of detected game moves (Fig. S.13a) and task performance (Fig. S.13b). Both environments can be solved with a high success rate of 94.9% (*LightsOutJaco*) and 96.3% (*LightsOut3DJaco*). For the experiments, we follow the evaluation protocols from the main paper.

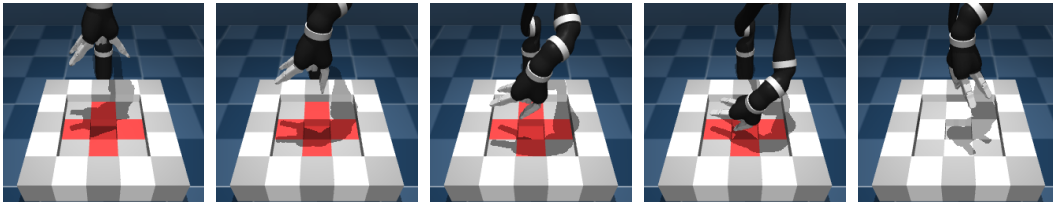
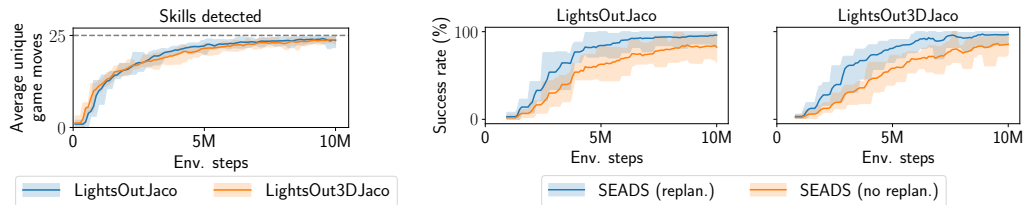


Figure S.12: *LightsOut3DJaco*: A variant of the *LightsOutJaco* environment with elevated fields. In comparison to the *LightsOutJaco* environment this environment poses an additional challenge to the agent, as it has to avoid to push fields with its fingers accidentally during skill execution. We show the execution of a skill which has learned to push the center field for $T = \{0, 4, 8, 12, 14\}$.

S.4.2 Larger LightsOut boards / spacing between fields

In this experiment we investigate how well SEADS performs on environments in which a very large number of skills has to be learned and where noisy executions of already learned skills uncover



(a) Average number of unique game moves detected on `LightsOutJaco` and `LightsOut3DJaco`. (b) SEADS task performance on `LightsOutJaco` and `LightsOut3DJaco`, with and without replanning.

Figure S.13: Evaluation on number of (a) detected game moves and (b) task performance on `LightsOut3DJaco` (see sec. S.4.1 for details).

new skills with low probability. To this end, we modified the `LightsOutCursor` environment to have more fields (and thereby, more skills to be learned), and introduced a spacing between the tiles, which makes detecting new skills more challenging. For a fair comparison, we keep the total actionable area in all environments constant, which introduces an empty area either around the board or around the tiles (see Fig. S.14). We make two main observations: (i) As presumed, learning skills in the `LightsOutCursor` environment with spacing between tiles requires more environment interactions than for adjacent tiles (see Fig. S.15a) (ii) For boards up to size 9×9 a large majority of skills is found after 1.5 million environment steps of training (5×5 : 24.9/25, 7×7 : 48.6/49, 9×9 : 76.8/81). The `LightsOutCursor` environment with boardsize 13×13 poses a challenge to SEADS with 119.3/169 skills detected after 1.5 million environment steps (see Fig. S.15). The numbers reported are averages over 5 independently trained agents.

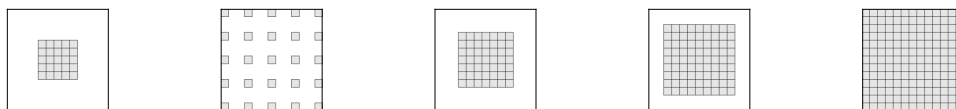


Figure S.14: Variants of `LightsOutCursor` for different board sizes (5×5 , 7×7 , 9×9 , 13×13) and spacing introduced between fields (second panel from left).

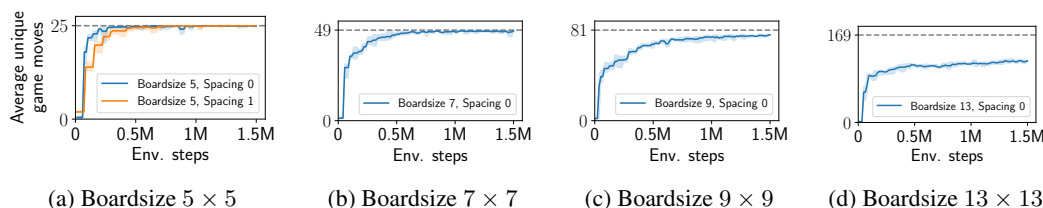


Figure S.15: Detected average unique game moves (skills) on `LightsOutCursor` environment for different board sizes (5×5 , 7×7 , 9×9 , 13×13) and spacing. The introduced spacing slows down skill learning (a). While for boards until size 9×9 nearly all skills are found (a-c), the 13×13 environment poses a challenge to SEADS (d). Solid line: mean / Shaded area: min/max over 5 independently trained agents.

S.5 Real Robot Experiment

For the real robot experiment we use a uArm Swift Pro robotic arm that interacts with a `LightsOut` board game. The board game runs on a Samsung Galaxy Tab A6 Android tablet with a screen size of 10.1 inches. We mapped the screen plane excluding the system status bar and action bar of the app (blue bar) to normalized coordinates $(x, y) \in [0, 1]$. A third $z \in [0, 1]$ coordinate measures the perpendicular distance to the screen plane, with $z = 1$ approximately corresponding to a distance

of 10 cm to the screen. To control the robot arm, we use the Python SDK from [2], which allows to steer the end effector to $\vec{X} = (X, Y, Z)$ target locations in a coordinate frame relative to the robot’s base. As the robot’s base is not perfectly aligned with the tablet’s surface, e.g. due to the rear camera, we employed a calibration procedure. We measured the location of the four screen corners in (X, Y, Z) coordinates using the SDK’s `get_position` method (by placing the end effector holding the capacitive pen on the particular corners) and fitted a plane to these points minimizing the squared distance. We reproject the measured points onto the plane and compute a perspective transform by pairing the reprojected points with normalized coordinates $(x, y) \in \{0, 1\} \times \{0, 1\}$. To obtain robot coordinates $(\hat{X}, \hat{Y}, \hat{Z})$ from normalized coordinates (x, y, z) we first apply the perspective transform on (x, y) , yielding $\hat{X} = (X, Y, Z = 0)$. We subsequently add the plane’s normal to (X, Y, Z) scaled by z and an additional factor which controls the distance to the tablet’s surface for $z = 1$. The state of the board is communicated to the host machine running SEADS via USB through the logging functionality of the Android Debug Bridge. The whole system including robotic arm and Android tablet is interfaced as an OpenAI Gym [3] environment.

S.5.1 Training on robot with absolute push position actions

In a first variant, the action space of the robotic environment is 2-dimensional, comprising a normalized pushing coordinate $(x, y) \in [0, 1]$ which is translated into a sequence of three commands sent to the robot, setting the position of the end effector to $(x, y, z = 0.2)$, $(x, y, z = 0)$, $(x, y, z = 0.2)$ subsequently. To simulate a more realistic gameplay, we do not resample the LightsOut board state or the robots’ pose at the beginning of an episode. We show the setup and behaviour during training in Fig. S.16. After 5000 environment interactions (corresponding to ≈ 7.5 hours total training time) we evaluated the SEADS agent’s performance on 100 board configurations (20 per solution depth in $\{1, \dots, 5\}$) and found all of them to be successfully solved by the agent.

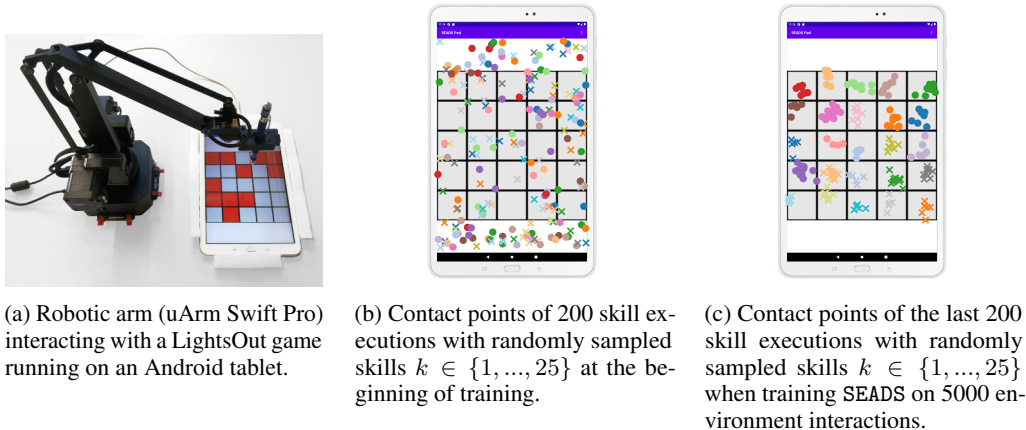


Figure S.16: Real-world setup with a robotic arm (a), on which SEADS learns a symbolic forward model on the LightsOut board state and associated low-level skills which relate to pushing locations on the tablet’s surface. In (b) and (c) we depict the first 200 and last 200 pushing locations of 5000 pushes used for training in total. While pushing locations are randomly scattered at the beginning of training (b), in the last 200 of 5000 training interactions skills relate to pushing particular fields on the game board (c).

S.5.2 Training on robot with positional displacement actions

In this experiment the action space of the environment is 3-dimensional $a = (\Delta x, \Delta y, p)$, with the first two actions being positional displacement actions $\Delta x, \Delta y \in [-0.2, 0.2]$ and the third action $p \in [-1, 1]$ indicating whether a ”push” should be executed. The displacement actions represent incremental changes to the robotic arm’s end effector position. In normalized coordinates (see sec. S.5) the end effector is commanded to steer to $(\text{clip}(x + \Delta x, 0, 1), \text{clip}(y + \Delta y, 0, 1), z = 0.3)$, where (x, y) are the current coordinates of the end effector. If the push action p exceeds a threshold $p > 0.6$, first the end effector is displaced, followed by a push, which is performed by sending the

target coordinates $(x, y, z = 0)$, $(x, y, z = 0.3)$ to the arm subsequently. In contrast to the first variant in which the SEADS agent sends a push location to the agent directly, here the SEADS agent has to learn temporally extended skills which first locate the end effector above a particular board field and then execute the push. Therefore, to reach a high success rate on the *LightsOut* task, significantly more environment interactions are required compared to the first variant. We observe that a test set of 25 *LightsOut* instances (5 per solution depth in $\{1, \dots, 5\}$) is solved with a success rate of 100% after $\approx 165k$ environment interactions, taking in total ≈ 43.5 hours wall-time to train. We refer to Fig. S.17 for a visualization of the success rate of SEADS over the course of training and to Fig. S.18 for a visualization of skills learned after $\approx 220k$ environment interactions. We refer to the project page at <https://seads.is.tue.mpg.de/> for a video on the real robot experiment.

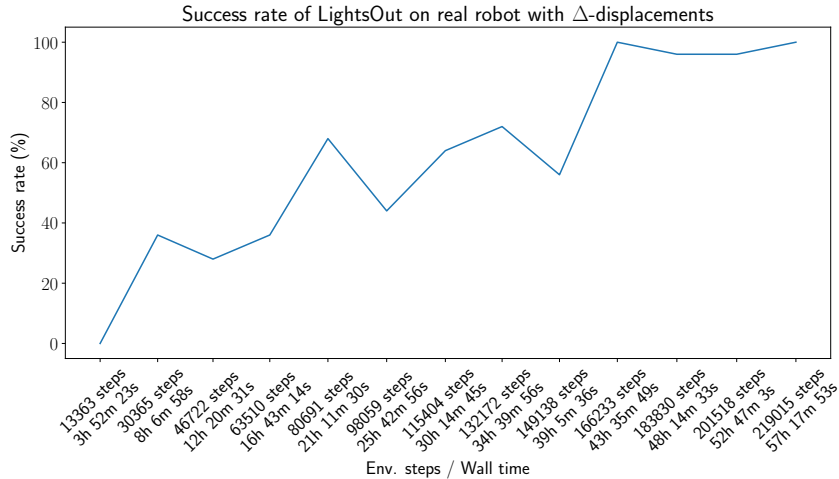


Figure S.17: Task success rate during the course of training SEADS on the *LightsOut* game embedded into a physical manipulation scenario with the uArm Swift Pro robotic arm. The arm is controlled by SEADS with positional displacement actions (see S.5.2). We evaluate the task performance as success rate on 25 board configurations for each reported step (5 instances per solution depth in $\{1, \dots, 5\}$).

S.6 Extended ablations

In this section we present an extended ablation analysis. We refer to sec. 4 of the main paper for a description of the evaluation protocol.

S.6.1 Relabelling

In this section we provide additional ablations for the episode relabelling. In addition to the "No relabelling" ablation considered in the main paper we investigate not relabelling episodes for the SAC agent only (No SAC relabelling) and not relabelling episodes for training the forward model (No forw. model relabelling). All evaluations are performed on 10 individually trained agents. We refer to Fig. S.19 for a visualization of the results. The results demonstrate that relabelling both for the forward model and SAC agent training are important for the performance of SEADS.

S.6.2 Numerical results

In Table S.1 we present the number of average unique game moves executed as skills by SEADS and its ablations. On the simpler Cursor environments, the ablations perform similarly well as SEADS in finding almost all skills. On the Reacher environments, most important for the performance of SEADS is to perform relabelling. On *LightsOut*Jaco, all ablated design choices are important for the high performance of SEADS.

We also observe that the "More skills" variant (equivalent to SEADS, but with $K = 30$ for *LightsOut*, $K = 15$ for *TileSwap*) yields a similar number of executed unique game moves as SEADS, which is

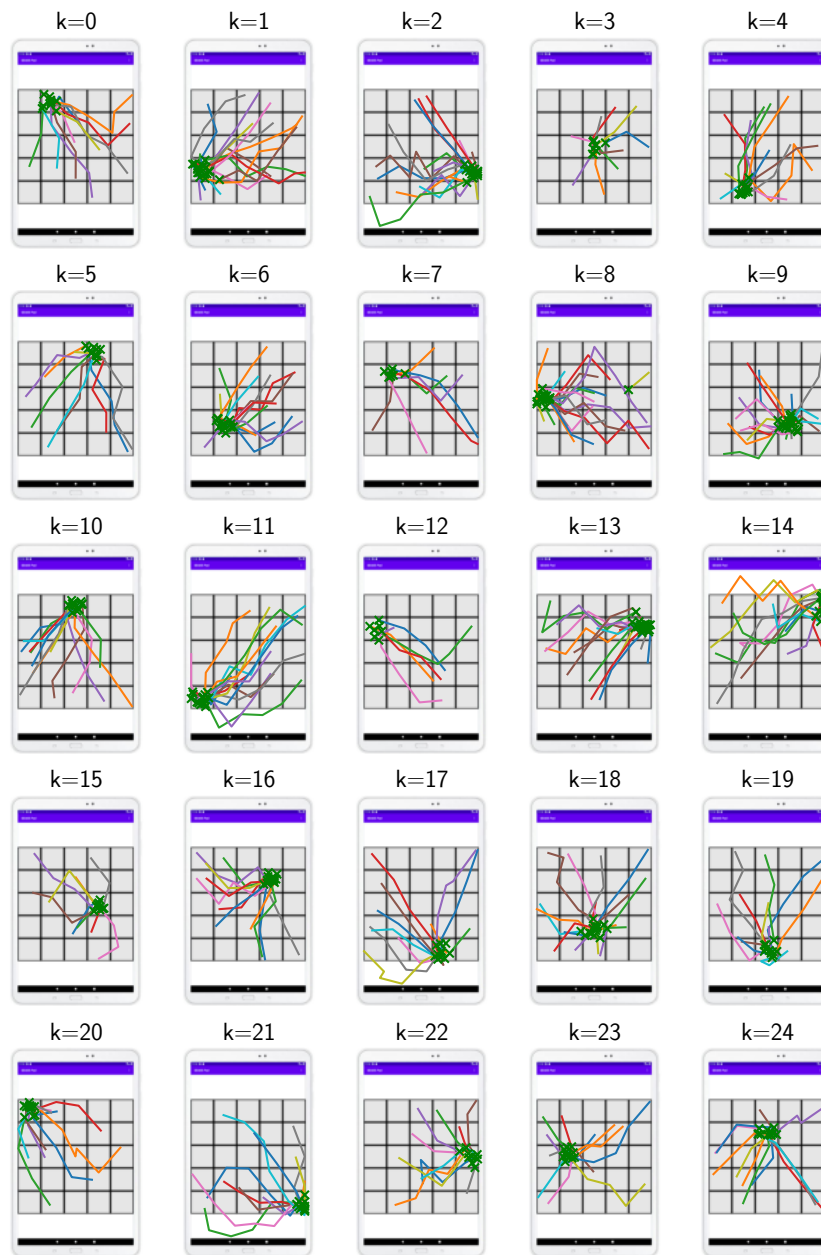


Figure S.18: Visualization of 320 trajectories executed on the uArm Swift robotic arm with positional displacement actions, after the agent has been trained for $\approx 220k$ environment interactions. Each subpanel shows trajectories for a specific symbolic action k . Green markers indicate push locations. Similar to the other environments, SEADS has learned to push individual fields as skills.

an encouraging result, justifying to over-estimate the number of skills K in situations where it is unknown.

We perform one-sided Mann-Whitney U tests [4] to conclude about significance of our results. On each environment, for each of the 10 independently trained SEADS agents, we obtain a set of 10 samples on the average number of detected skills. Analogously, we obtain such a set of 10 samples for every ablation. We aim at finding ablations which either (i) detect significantly more skills than SEADS or (ii) detect significantly less skills than SEADS on a particular environment. We reject null hypotheses for $p < 0.01$. For (i), we first set up the null hypothesis that the distribution

underlying the SEADS samples is stochastically greater or equal to the distribution underlying the ablation samples. For ablations on which this null hypothesis can be rejected it holds that they detect significantly more skills than SEADS. *As we cannot reject the null hypothesis for any ablation, no ablation exists which detects significantly more skills than SEADS.* For (ii), we set up the null hypothesis that the distribution underlying the SEADS samples is stochastically less or equal to the distribution underlying the ablation samples. *For all ablations there exists at least one environment in which we can reject the null hypothesis to (ii), indicating that all ablations contribute significantly to the performance of SEADS on at least one environment.* The results of the significance test are highlighted in Table S.1.

	Cursor		Reacher		Jaco	
	LightsOut	TileSwap	LightsOut	TileSwap	LightsOut	TileSwap
SEADS	24.94 ± 0.06	11.99 ± 0.02	24.3 ± 0.28	11.81 ± 0.13	23.64 ± 1.04	11.54 ± 0.27
No sec.-best norm.	24.74 ± 0.42	11.98 ± 0.03	24.42 ± 0.32	11.78 ± 0.11	22.28 ± 0.92	9.26 ± 1.17
No nov. bonus	24.83 ± 0.32	11.99 ± 0.03	23.75 ± 0.71	11.81 ± 0.09	20.24 ± 1.46	11.58 ± 0.29
No relab.	24.72 ± 0.39	12.0 ± 0.02	16.58 ± 4.62	3.62 ± 3.2	19.26 ± 1.0	11.53 ± 0.12
No forw. mod. relab.	24.9 ± 0.07	11.99 ± 0.02	22.73 ± 0.94	11.77 ± 0.28	11.5 ± 3.47	8.64 ± 1.83
No SAC relabelling	24.88 ± 0.09	11.98 ± 0.03	22.94 ± 1.51	11.76 ± 0.15	17.32 ± 2.54	11.05 ± 0.48
More skills	24.97 ± 0.03	11.99 ± 0.02	24.36 ± 0.36	11.8 ± 0.12	23.9 ± 0.47	11.47 ± 0.41

Table S.1: Number of average unique game moves executed as skills by SEADS and its ablations, with a maximum of 5×10^5 (*Cursor*) / 1×10^7 (*Reacher, Jaco*) environment interactions (see Sec. S.8.1 for details). The ablated design choices contribute to the performance of SEADS especially on the more difficult *Reacher* and *Jaco* environments. Overestimating the number of skills does not decrease performance (“More skills”). We report mean and standard deviation on 10 independently trained agents. Ablations which perform significantly (one-sided Mann-Whitey U [4], $p < 0.01$) worse than SEADS are colored red. We did not find any ablation to perform significantly better than SEADS (including the “More skills” ablation). We refer to sec. S.6.2 for details.

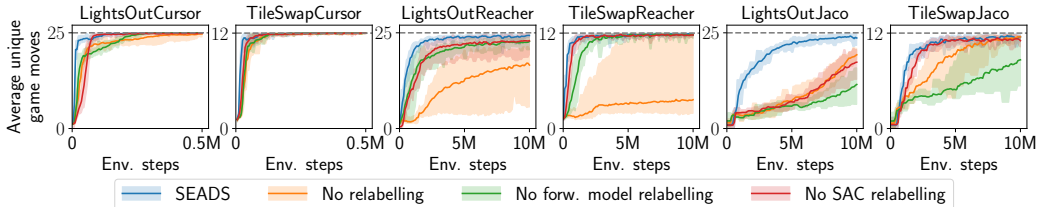


Figure S.19: Extended relabelling ablation analysis with 10 trained agents per variant. The results demonstrate that relabelling both for the forward model and SAC agent training are important for the performance of SEADS. See sec. S.6 for details.

S.7 Environment details

S.7.1 Cursor environments

At the beginning of an episode, the position of the cursor is reset to $x \sim \text{Uniform}(0, 1)$, $y \sim \text{Uniform}(0, 1)$. After a game move, the cursor is not reset. Both *LightsOut* and *TileSwap* board extents are $(x, y) \in [0, 1] \times [0, 1]$.

S.7.2 Reacher environments

At the beginning of an episode, the two joints of the Reacher are set to random angles $\theta \sim \text{Uniform}(0, 2\pi)$, $\phi \sim \text{Uniform}(0, 2\pi)$. After a game move, the joints are not reset. Both *LightsOut* and *TileSwap* board extents are $(x, y) \in [-0.15, 0.15] \times [-0.15, 0.15]$. The control simulation timestep is 0.02s, and we use an action repeat of 2.

Algorithm 1 Task solution (without replanning). `bfs_plan` denotes breadth-first search over a sequence of skills to transition $z_{(0)}$ to z^* , leveraging the symbolic forward model q_θ . Nodes are expanded in BFS via the function $\text{successor}_{q_\theta} : \mathcal{Z} \times \mathcal{K} \rightarrow \mathcal{Z}$.

Input: environment E , skill-conditioned policy π , symbolic forward model q_θ , initial state $s_{(0)} = s_0$, symbolic goal z^* , symbolic mapping function Φ
Output: boolean success
 $N, [k_1, \dots, k_N] = \text{bfs_plan}(q_\theta, z_{(0)} = \Phi(s_{(0)}), z^*)$
for $n = 1$ **to** N **do**
 $s_{(n)} = \text{apply}(E, \pi, s_{(n-1)}, k_i)$
end for
success = $(\Phi(s_{(N)}) == z^*)$

S.7.3 Jaco environments

At the beginning of an episode and after a game move the Jaco arm is randomly reset above the board. The tool’s (end effector) center point is randomly initialized to $x \sim \text{Uniform}(-0.1, 0.1)$, $y \sim \text{Uniform}(-0.1, 0.1)$, $z \sim \text{Uniform}(0.2, 0.4)$ with random rotation $\theta \sim \text{Uniform}(-\pi, \pi)$. The *LightsOut* board extent is $(x, y) \in [-0.25, 0.25] \times [-0.25, 0.25]$, the *TileSwap* board extent $(x, y) \in [-0.15, 0.15] \times [-0.15, 0.15]$. We use a control timestep of $0.1s$ in the simulation.

S.8 SEADS details

In the following, we will present algorithmic and architectural details of our approach.

S.8.1 Checkpointing

The number of environment steps varies per model checkpoint due to varying skill lengths. We report results for budgets of environments steps as the results of model checkpoints being below this threshold.

For the *Skill learning evaluation*, i.e., the average number of detected game moves, we report results on the last checkpoints before reaching $5 \cdot 10^5$ (*Cursor*), 10^7 (*Reacher, Jaco*) env. steps. The results are reported for checkpoints taken after $4.95 \cdot 10^5$ (*Cursor*), $9.89 \cdot 10^6$ (*Reacher, Jaco*) env. steps on average.

For the *Planning evaluation*, i.e., the success rate, we again limit the number of environment steps to $5 \cdot 10^5$ (*Cursor*), 10^7 (*Reacher, Jaco*). We determine results at the last checkpoints for which, for every seed, at least one checkpoint exists with the same or higher number of environment steps (i.e., the last common checkpoints). Effectively, these results are obtained at checkpoints with an average number of $4.76 \cdot 10^5$ (*Cursor*), $9.34 \cdot 10^6$ (*Reacher, Jaco*) env. steps.

S.8.2 Task solution with and without replanning

One main idea of the proposed SEADS agent is to use separate phases of symbolic planning (using the symbolic forward model $q_\theta(z_T | z_0, k)$) and low-level control (using the skill policies $\pi(a | s, k)$) for solving tasks. In algorithm 1 and algorithm 2 we present pseudocode of task solution using planning and skill execution, with and without intermittent replanning.

S.8.3 Training procedure

The main training loop of our proposed SEADS agent consists of intermittent episode collection and re-labelling for training the skill-conditioned policy π using soft actor-critic (SAC, [5]) and symbolic forward model (see Algorithm 3). For episode collection we first sample a skill from a uniform distribution over skills $k \sim \text{Uniform}\{1, \dots, K\}$ and then collect the corresponding episode. In our experiments we collect 32 episodes per epoch (i.e., $N_{\text{episodes}} = 32$) for all experiments except the real robot experiment with absolute push positions (sec. S.5.1), where we collect 4 episodes per epoch. We maintain two replay buffers of episodes for short-term ($\text{Episodes}_{\text{recent}}$) and long-term storage ($\text{Episodes}_{\text{buffer}}$), in which we keep the $N_{\text{buffer}} = 2048 / N_{\text{recent}} = 256$ most recent

Algorithm 2 Task solution (with replanning). `bfs_plan` denotes breadth-first search over a sequence of skills to transition $z_{(0)}$ to z^* , leveraging the symbolic forward model q_θ . Nodes are expanded in BFS via the function `successor $_{q_\theta}$` : $\mathcal{Z} \times \mathcal{K} \rightarrow \mathcal{Z}$.

Input: environment E , skill-conditioned policy π , symbolic forward model q_θ , initial state $s_{(0)} = s_0$, symbolic goal z^* , symbolic mapping function Φ
 $n \leftarrow 0$
repeat
 $N, [k_1, \dots, k_N] \leftarrow \text{bfs_plan}(q_\theta, z_{(n)} = \Phi(s_{(n)}), z^*)$
for $i \in \{1, \dots, N\}$ **do**
 $n \leftarrow n + 1$
 $\hat{z}_{(n)} \leftarrow \text{successor}_{q_\theta}(\Phi(s_{(n-1)}), k_i)$ {Compute the expected symbolic state after applying skill k_i }
 $s_{(n)} \leftarrow \text{apply}(E, \pi, s_{(n-1)}, k_i)$
 $z_{(n)} \leftarrow \Phi(s_{(n)})$
if $z_{(n)} \neq \hat{z}_{(n)}$ **then**
Break {If the actual symbolic state differs from the predicted state, we replan}
end if
end for
until $z_{(n)} == z^*$

episodes. For training the SAC agent and skill model we combine a sample of 256 episodes from the long-term buffer and all 256 episodes from the short-term buffer, comprising the episodes `Episodes`. These episodes are subsequently passed to the relabelling module. On these relabelled episodes the SAC agent and skill model are trained. Please see the following subsections for details on episode collection, relabelling, skill model training and policy training.

Algorithm 3 SEADS training loop

Input: Environment E
Number of epochs N_{epochs}
Number of new episodes per epoch N_{episodes}
Episode buffer size N_{buffer}
Result: Trained skill-conditioned policy $\pi(a | s, k)$ and forward model $q_\theta(z_T | z_0, k)$
`Episodes $_{\text{buffer}}$` = [], `Episodes $_{\text{recent}}$` = []
for $n_{\text{epoch}} = 1$ **to** N_{epochs} **do**
for $n_{\text{episode}} = 1$ **to** N_{episodes} **do**
Sample $k \sim p(k)$
 $s_0 = E.\text{reset}()$
 $\text{Ep} = \text{collect_episode}(E, \pi, s_0, k)$
`Episodes $_{\text{buffer}}$` .append(Ep), `Episodes $_{\text{recent}}$` .append(Ep)
end for
`Episodes $_{\text{buffer}}$` \leftarrow `Episodes $_{\text{buffer}}$` [- N_{buffer} :] {Keep N_{buffer} most recent episodes}
`Episodes $_{\text{recent}}$` \leftarrow `Episodes $_{\text{recent}}$` [- N_{recent} :]
`Episodes` = sample(`Episodes $_{\text{buffer}}$` , $N = 256$) \cup `Episodes $_{\text{recent}}$`
`Episodes $_{\text{SM}}$` \leftarrow relabel(`Episodes`, $p = 1.0$)
update_skill_model(`Episodes $_{\text{SM}}$`)
`Episodes` = sample(`Episodes $_{\text{buffer}}$` , $N = 256$) \cup `Episodes $_{\text{recent}}$`
`Episodes $_{\text{SAC}}$` \leftarrow relabel(`Episodes`, $p = 0.5$)
update_sac(`Episodes $_{\text{SAC}}$`)
end for

S.8.3.1 Episode collection (`collect_episode`)

The operator `collect_episode` works similar to the `apply` operator defined in the main paper (see sec. 3). It applies the skill policy $\pi(a_t | s_t, k)$ iteratively until termination. However, the operator returns all intermediate states s_0, \dots, s_T and actions a_0, \dots, a_{T-1} to be stored in the episode replay buffers.

S.8.3.2 Relabelling (relabel)

For relabelling we sample a Bernoulli variable with success probability of p for each episode in the Episodes buffer, indicating whether it may be relabeled. For training the forward model we relabel all episodes ($p = 1$), while for the SAC agent we only allow half of the episodes to be relabeled ($p = 0.5$). The idea is to train the SAC agent also on *negative* examples of skill executions with small rewards. Episodes in which the symbolic observation did not change are excluded from relabelling for the SAC agent, as for those the agent receives a constant negative reward. All episodes which should be relabeled are passed to the relabelling module as described in sec. 3. The union of these relabelled episodes and the episodes which were not relabeled form the updated buffer which is returned by the relabel operator.

S.8.3.3 SAC agent update (update_sac)

In each epoch, we fill a transition buffer using all transitions from the episodes in the Episodes_{SAC} buffer. Each transition tuple is of the form $([s_t^i, k^i], a_t^i, [s_{t+1}^i, k^i], r_{t+1}^i)$ where s are environment observations, a low-level actions, k a one-hot representation of the skill and r the intrinsic reward. $[\cdot]$ denotes the concatenation operation. The low-level SAC agent is trained for 16 steps per epoch on batches comprising 128 randomly sampled transitions from the transition buffer. We train the actor and critic networks using Adam [6]. For architectural details of the SAC agent, see sec. S.8.4.1.

S.8.3.4 Skill model update (update_skill_model)

From the episode buffer Episodes_{SM} we sample transition tuples $(z_0^i, k_i, z_{T^i}^i)$. The skill model is trained to minimize an expected loss

$$\mathcal{L} = \mathbb{E}_{\mathcal{B}} \left[\sum_{i \in \mathcal{B}} L(z_0^i, k_i, z_{T^i}^i) \right] \tag{2}$$

for randomly sampled batches \mathcal{B} of transition tuples. We optimize the skill model parameters θ using the Adam [6] optimizer for 4 steps per epoch on batches of size 32. We use a learning rate of 10^{-3} . The instance-wise loss L to be minimized corresponds to the negative log-likelihood $L = -\log q_{\theta}(z_{T^i}^i | z_0^i, k)$ for symbolic forward models or $L = -\log q_{\theta}(k | z_0^i, z_{T^i}^i)$ for the VIC ablation (see sec. S.11).

S.8.4 Architectural details

S.8.4.1 SAC agent

We use an open-source soft actor-critic implementation [7] in our SEADS agent. Policy and critic networks are modeled by a multilayer perceptron with two hidden layers with ReLU activations. For hyperparameters, please see the table below.

$\{LightsOut, TileSwap\}$ -	<i>Cursor</i>	<i>Reacher</i>	<i>Jaco</i>	Robot (LightsOut)
Learning rate	$3 \cdot 10^{-4}$	$3 \cdot 10^{-4}$	$3 \cdot 10^{-4}$	$3 \cdot 10^{-4}$
Target smoothing coeff. τ	0.005	0.005	0.005	0.005
Discount factor γ	0.99	0.99	0.99	0.99
Hidden dim.	512	512	512	512
Entropy target α	0.1	0.01	0.01	0.1
Automatic entropy tuning	no	no	no	no
Distribution over actions	Gaussian	Gaussian	Gaussian	Gaussian

S.8.4.2 Symbolic forward model

Our symbolic forward model models the distribution over the terminal symbolic observation z_T given the initial symbolic observation z_0 and skill k . It factorizes over the symbolic observation as $q_{\theta}(z_T | k, z_0) = \prod_{d=1}^D q_{\theta}([z_T]_d | k, z_0) = \prod_{d=1}^D \text{Bernoulli}([\alpha_T(z_0, k)]_d)$ where D is the dimensionality of the symbolic observation. We assume $z \in \mathcal{Z}$ to be a binary vector with $\mathcal{Z} = \{0, 1\}^D$. The Bernoulli probabilities $\alpha_T(z_0, k)$ are predicted by a learnable neural component. We use a neural

network f to parameterize the probability of the binary state in z_0 to flip $p_{\text{flip}} = f_{\theta}(z_0, k)$, which simplifies learning if the *change* in symbolic state only depends on k and is independent of the current state. Let α_T be the probability for the binary state to be True, then $\alpha_T = (1 - z_0) \cdot p_{\text{flip}} + z_0 \cdot (1 - p_{\text{flip}})$. The input to the neural network is the concatenation $[z_0, \text{onehot}(k)]$. We use a multilayer perceptron with two hidden layers with ReLU nonlinearities and 256 hidden units.

S.9 SAC baseline

We train the SAC baseline in a task-specific way by giving a reward of 1 to the agent if the board state has reached its target configuration and 0 otherwise. At the beginning of each episode we first sample the difficulty of the current episode which corresponds to the number of moves required to solve the game (solution depth S). For all environments S is uniformly sampled from $\{1, \dots, 5\}$. For all *Cursor* environments we impose a step limit $T_{\text{lim}} = 10 \cdot S$, for *Reacher* and *Jaco* $T_{\text{lim}} = 50 \cdot S$. This corresponds to the number of steps a single skill can make in SEADS multiplied by S . We use a replay buffer which holds the most recent 1 million transitions and train the agent with a batchsize of 256. The remaining hyperparameters (see table below) are identical to the SAC component in SEADS; except for an increased number of hidden units and an additional hidden layer (i.e., three hidden layers) in the actor and critic networks to account for the planning the policy has to perform. In each epoch of training we collect 8 samples from each environment which we store in the replay buffer. We performed a hyperparameter search on the number of agent updates performed in each epoch N and entropy target values α . We also experimented with skipping updates, i.e., collecting 16 (for $N = 0.5$) or 32 (for $N = 0.25$) environment samples before performing a single update. We found that performing too many updates leads to unstable training (e.g., $N = 4$ for *LightsOutCursor*). For all results and optimal settings per environment, we refer to sec. S.13.1. For the SAC baseline we use the same SAC implementation from [7] which we use for SEADS.

$\{\textit{LightsOut}, \textit{TileSwap}\}$ -	<i>Cursor</i>	<i>Reacher</i>	<i>Jaco</i>
Learning rate	$3 \cdot 10^{-4}$	$3 \cdot 10^{-4}$	$3 \cdot 10^{-4}$
Target smoothing coeff. τ	0.005	0.005	0.005
Discount factor γ	0.99	0.99	0.99
Hidden dim.	512	512	512
Entropy target α	<i>tuned</i> (see sec. S.13.1)		
Automatic entropy tuning	no	no	no
Distribution over actions	Gaussian	Gaussian	Gaussian

S.10 HAC baseline

For the HAC baseline we adapt the official code release [8]. We modify the architecture to allow for a two-layer hierarchy of policies in which the higher-level policy commands the lower-level policy with *discrete* subgoals (which correspond to the symbolic observations z in our case). This requires the higher-level policy to act on a discrete action space $\mathcal{A}_{\text{high}} = \mathcal{Z}$. The lower-level policy acts on the continuous actions space $\mathcal{A}_{\text{low}} = \mathcal{A}$ of the respective manipulator (*Cursor*, *Reacher*, *Jaco*). To this end, we use a discrete-action SAC agent for the higher-level policy and a continuous-action SAC agent for the lower-level policy. For the higher-level discrete SAC agent we parameterize the distribution over actions as a factorized reparametrizable RelaxedBernoulli distribution, which is a special case of the Concrete [9] / Gumbel-Softmax [10] distribution. We use an open-source SAC implementation [7] for the SAC agent on both levels and extend it by a RelaxedBernoulli distribution over actions for the higher-level policy.

S.10.1 Hyperparameter search

We performed an extensive hyperparameter search on all 6 environments ($[\textit{LightsOut}, \textit{TileSwap}] \times [\textit{Cursor}, \textit{Reacher}, \textit{Jaco}]$) for the HAC baseline. We investigated a base set of entropy target values $\alpha_{\text{low}}, \alpha_{\text{high}} \in \{0.1, 0.01, 0.001, 0.0001\}$ for both layers separately. On the *Cursor* environments we refined these sets in regions of high success rates. We performed a hyperparameter search on the temperature parameter τ of the RelaxedBernoulli distribution on the *Cursor* environments with $\tau \in \{0.01, 0.05, 0.1, 0.5\}$ and found $\tau = 0.1$ to yield the best results. For experiments on the *Reacher*

and *Jaco* environments we then fixed the parameter $\tau = 0.1$. We report results on parameter sets with highest average success rate on 5 individually trained agents after 5×10^5 (*Cursor*) / 1×10^7 (*Reacher*, *Jaco*) environment interactions. We refer to sec. S.13.2 for a visualization of all hyperparameter search results.

Parameters for high-level policy

<i>all environments</i>	
Learning rate	$3 \cdot 10^{-4}$
Target smoothing coeff. τ	0.005
Discount factor γ	0.99
Hidden layers for actor/critic	2
Hidden dim.	512
Entropy target α_{high}	<i>tuned</i> (see sec. S.13.2)
Automatic entropy tuning	no
Distribution over actions	RelaxedBernoulli
RelaxedBernoulli temperature τ	<i>tuned</i> (see sec. S.13.2)

Parameters for low-level policy

<i>all environments</i>	
Learning rate	$3 \cdot 10^{-4}$
Target smoothing coeff. τ	0.005
Discount factor γ	0.99
Hidden layers for actor/critic	2
Hidden dim.	512
Entropy target α_{high}	<i>tuned</i> (see sec. S.13.2)
Automatic entropy tuning	no
Distribution over actions	Gaussian

S.11 VIC baseline

We compare to Variational Intrinsic Control (VIC, Gregor et al. [1]) as a baseline method of unsupervised skill discovery. It is conceptually similar to our method as it aims to find skills such that the mutual information $\mathcal{I}(s_T, k | s_0)$ between the skill termination state s_T and skill k is maximized given the skill initiation state s_0 . To this end it jointly learns a skill policy $\pi(s_t | a_t, k)$ and *skill discriminator* $q_\theta(k | s_0, s_T)$. We adopt this idea and pose a baseline to our approach in which we model $q_\theta(k | z_0, z_T)$ *directly* with a neural network, instead of modelling $q_\theta(k | z_0, z_T)$ indirectly through a forward model $q_\theta(z_T | z_0, k)$. The rest of the training process including its hyperparameters is identical to SEADS. We implement $q_\theta(k | z_0, z_T)$ by a neural network which outputs the parameters of a categorical distribution and is trained by maximizing the log-likelihood $\log q_\theta(k | z_0^i, z_{T,i}^i)$ on transition tuples $(z_0^i, k_i, z_{T,i}^i)$ (see sec. S.8.3.4). We experimented with different variants of passing $(z_0^i, z_{T,i}^i)$ to the network: (i) concatenation $[z_0^i, z_{T,i}^i]$ and (ii) concatenation with XOR $[z_0^i, z_{T,i}^i, z_0^i \text{ XOR } z_{T,i}^i]$. We only found the latter to show success during training. The neural network model contains two hidden layers of size 256 with ReLU activations (similar to the forward model). We also evaluate variants of VIC which are extended by our proposed *relabelling scheme* and *second-best reward normalization*. In contrast to VIC, our SEADS agent discovers all possible game moves reliably in both `LightsOutCursor` and `TileSwapCursor` environments, see Fig. S.20 for details. Our proposed second-best normalization scheme (+*SBN*, sec. 3) slightly improves performance of VIC in terms of convergence speed (`LightsOutCursor`) and variance in number of skills detected (`TileSwapCursor`). The proposed relabelling scheme (+*RL*, sec. 3) does not improve (`LightsOutCursor`) or degrades (`TileSwapCursor`) the number of detected skills.

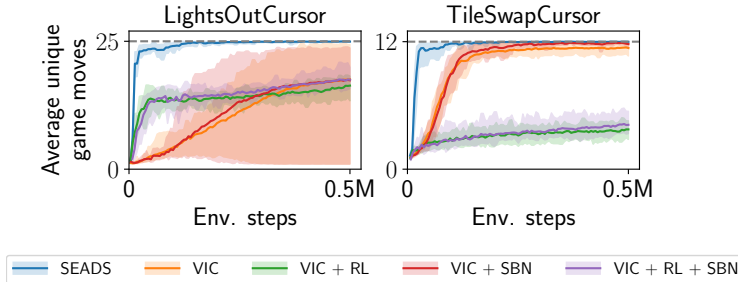


Figure S.20: Number of discovered skills on the `LightsOutCursor`, `TileSwapCursor` environments for the SEADS agent and variants of VIC [1]. Only SEADS discovers all skills reliably on both environments. See sec. S.11 for details.

	solution depth							
	1	2	3	4	5	6	7	8
LightsOut	25	300	2300	12650	53130	176176	467104	982335
TileSwap	12	88	470	1978	6658	18081	38936	65246
	solution depth							
	9	10	11	12	13	14	15	16
LightsOut	1596279	1935294	1684446	1004934	383670	82614	7350	0
TileSwap	83000	76688	48316	18975	4024	382	24	1

Table S.2: Number of feasible board configurations for varying solution depths. No feasible board configurations exist with solution depth > 16 .

S.12 Environment details

S.12.1 Train-/Test-split

In order to ensure disjointness of board configurations in train and test split we label each board configuration based on a hash remainder. For the hashing algorithm we first represent the current board configuration as comma-separated string, e.g. $s = "1, 1, 0, \dots, 0"$ for `LightsOut` and $s = "1, 0, 2, \dots, 8"$ for `TileSwap`. Then, this string is passed through a CRC32 hashing function, yielding the split based on an integer division remainder

$$\text{split} = \begin{cases} \text{train} & \text{CRC32}(s) \bmod 3 = 0 \\ \text{test} & \text{CRC32}(s) \bmod 3 \in \{1, 2\} \end{cases} \quad (3)$$

S.12.2 Board initialization

We quantify the difficulty of a particular board configuration by its *solution depth*, i.e., the minimal number of game moves required to solve the board.

We employ a breadth-first search (BFS) beginning from the goal board configuration (all fields *off* in `LightsOut`, ordered fields in `TileSwap`). Nodes (board configurations) are expanded through applying feasible actions (12 for `TileSwap`, 25 for `LightsOut`). Once a new board configuration is observed for the first time, its solution depth corresponds to the current BFS step.

By this, we find all feasible board configurations for `LightsOut` and `TileSwap` and their corresponding solution depths (see table S.2). In table S.3 we show the sizes of the training and test split for `LightsOut` and `TileSwap` environments for solution depths in $\{1, \dots, 5\}$.

		solution depth				
		1	2	3	4	5
LightsOut	train	7	99	785	4200	17849
	test	18	201	1515	8450	35281
	total	25	300	2300	12650	53130
TileSwap	train	7	31	179	683	2237
	test	5	57	291	1295	4421
	total	12	88	470	1978	6658

Table S.3: Number of initial board configurations for varying solution depths and dataset splits (train / test).

S.13 Results of hyperparameter search on HAC and SAC baselines

S.13.1 Results of SAC hyperparameter search

Please see figures S.21, S.22, S.23, S.24, S.25, S.26 for a visualization of the SAC hyperparameter search results.

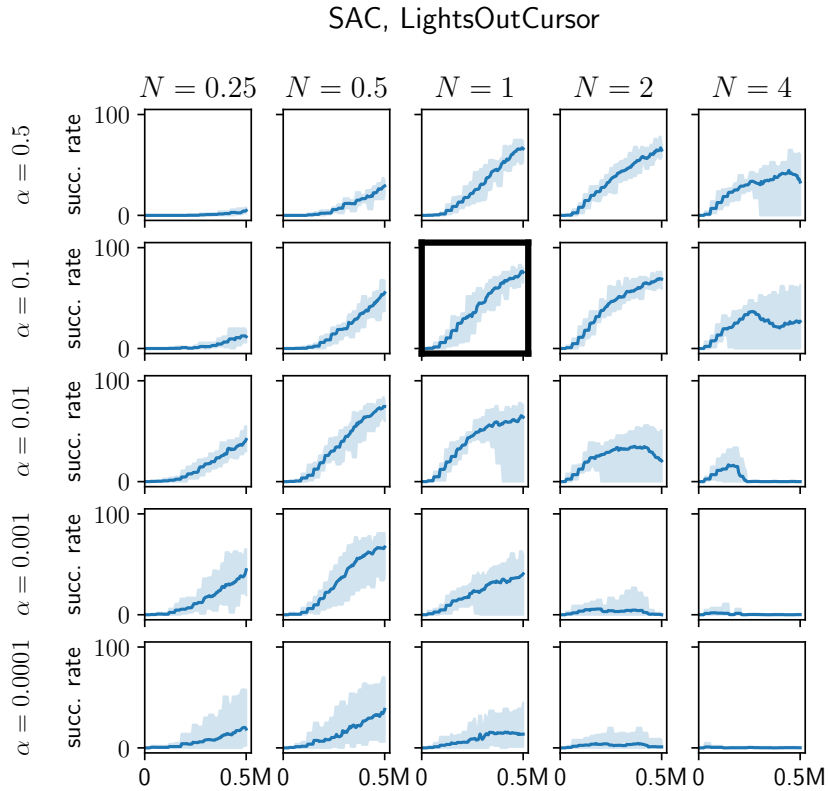


Figure S.21: Test performance of SAC agents on the LightsOutCursor environment for varying number of update steps per epoch (N) and parameters α . We evaluate 5 individual agents per configuration. The best configuration is marked in **bold** ($N = 1, \alpha = 0.1$).

SAC, TileSwapCursor

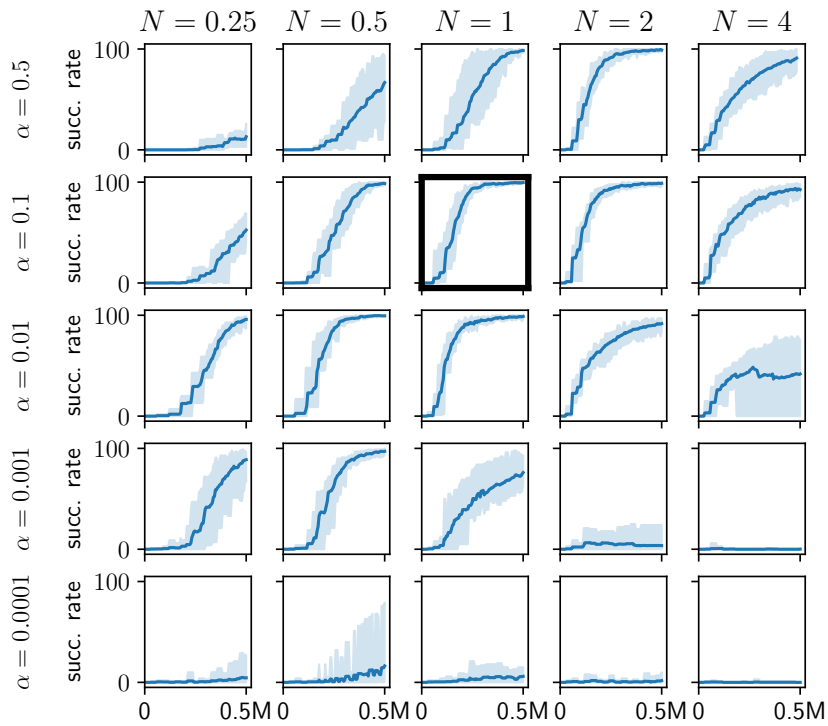


Figure S.22: Test performance of SAC agents on the TileSwapCursor environment for varying number of update steps per epoch (N) and parameters α . We evaluate 5 individual agents per configuration. The best configuration is marked in **bold** ($N = 1$, $\alpha = 0.1$).

SAC, LightsOutReacher

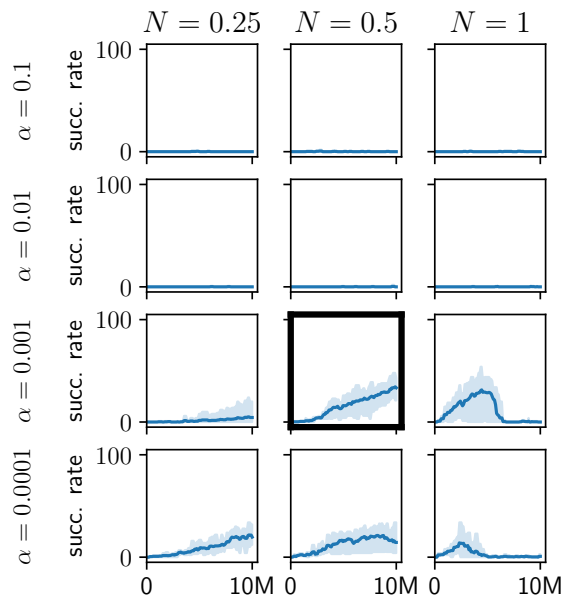


Figure S.23: Test performance of SAC agents on the LightsOutReacher environment for varying number of update steps per epoch (N) and parameters α . We evaluate 5 individual agents per configuration. The best configuration is marked in **bold** ($N = 0.5$, $\alpha = 0.001$).

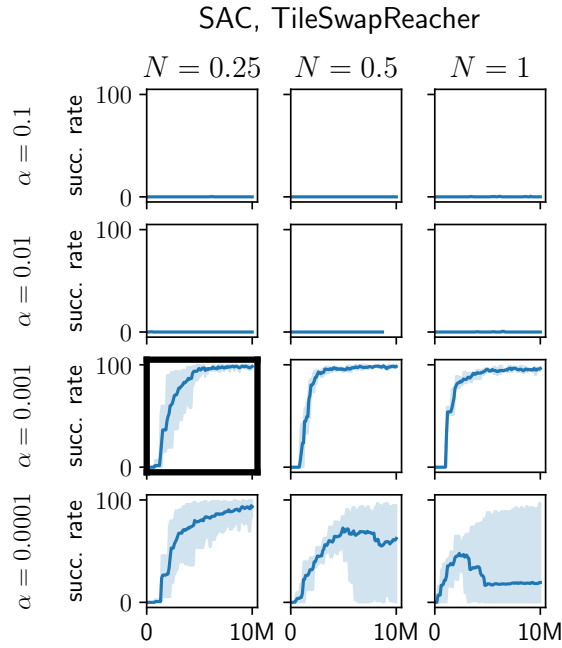


Figure S.24: Test performance of SAC agents on the TileSwapReacher environment for varying number of update steps per epoch (N) and parameters α . We evaluate 5 individual agents per configuration. The best configuration is marked in **bold** ($N = 0.25$, $\alpha = 0.001$).

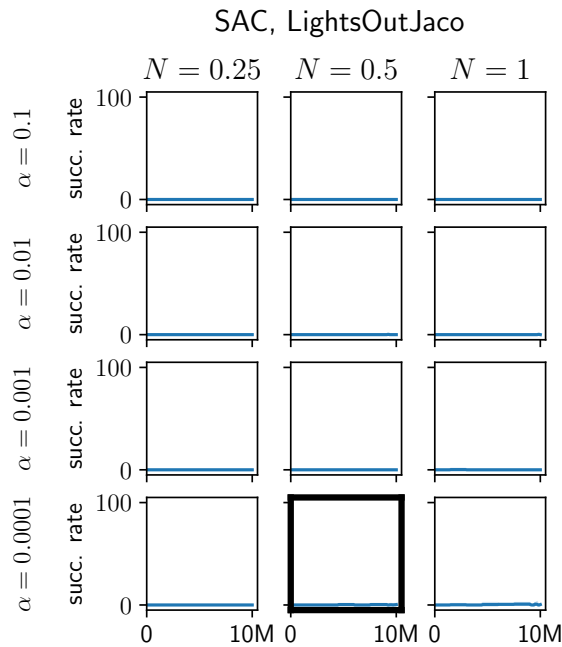


Figure S.25: Test performance of SAC agents on the LightsOutJaco environment for varying number of update steps per epoch (N) and parameters α . We evaluate 5 individual agents per configuration. The best configuration is marked in **bold** ($N = 0.5$, $\alpha = 0.0001$).

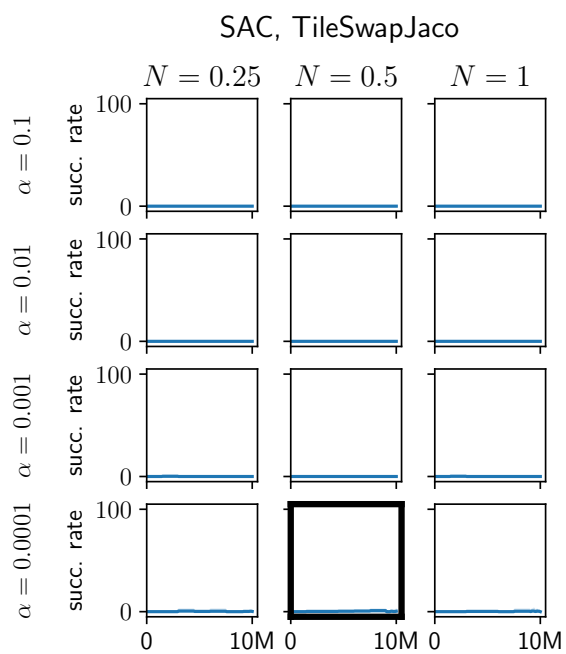
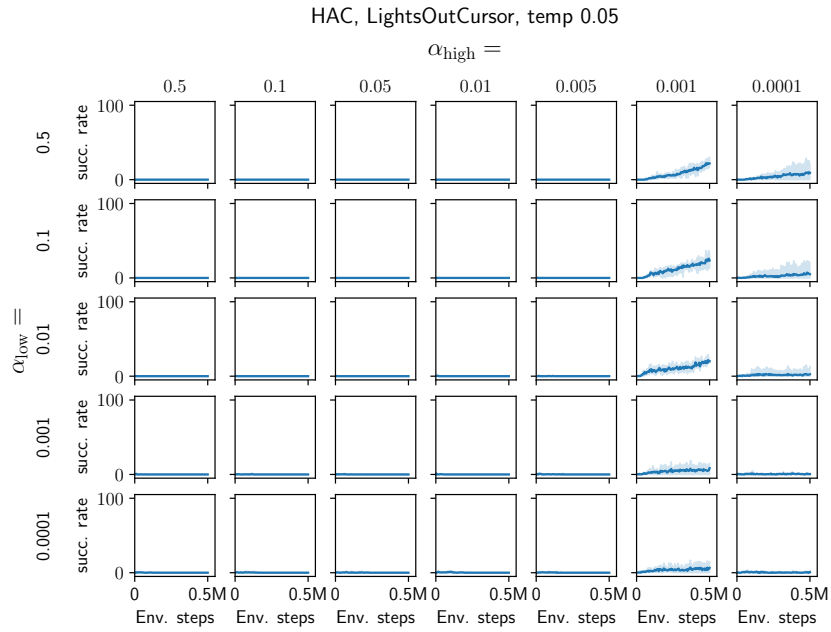
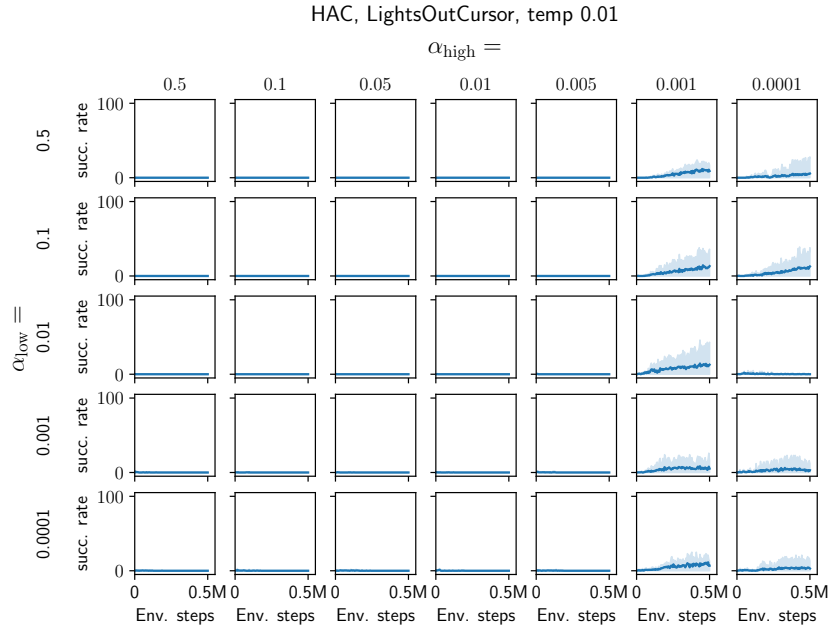


Figure S.26: Test performance of SAC agents on the TileSwapJaco environment for varying number of update steps per epoch (N) and parameters α . We evaluate 5 individual agents per configuration. The best configuration is marked in **bold** ($N = 0.5$, $\alpha = 0.0001$).

S.13.2 Results of HAC hyperparameter search

Please see figures S.26, S.26, S.27, S.28, S.29, S.30 for a visualization of the HAC hyperparameter search results.



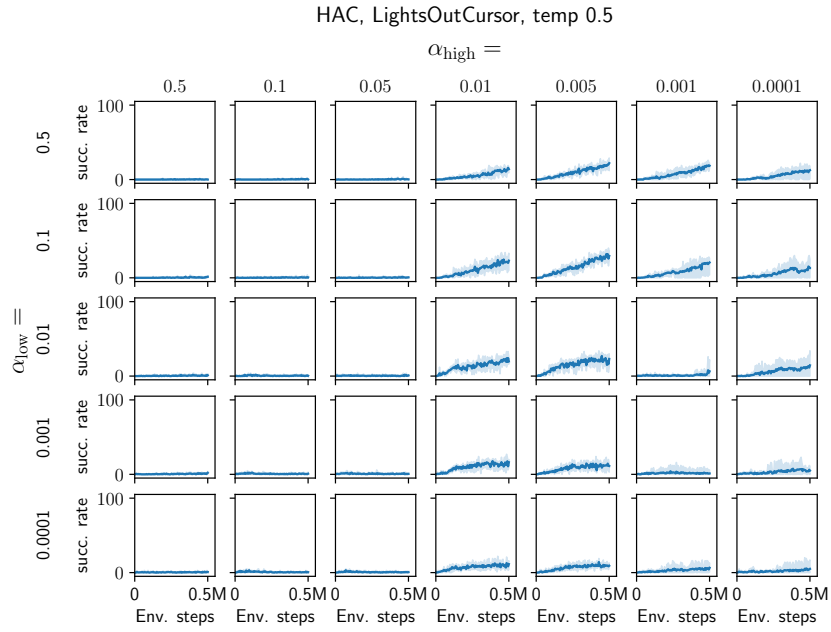
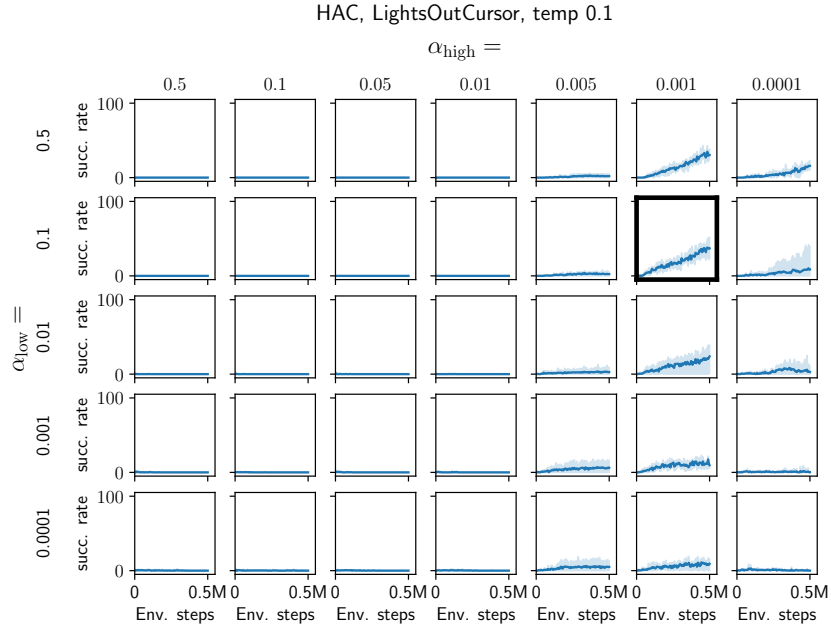
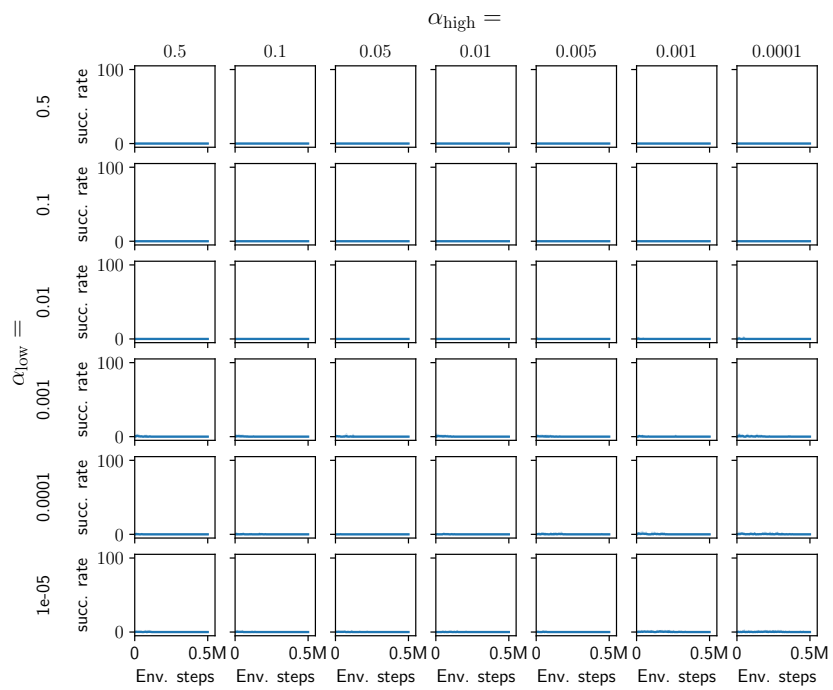
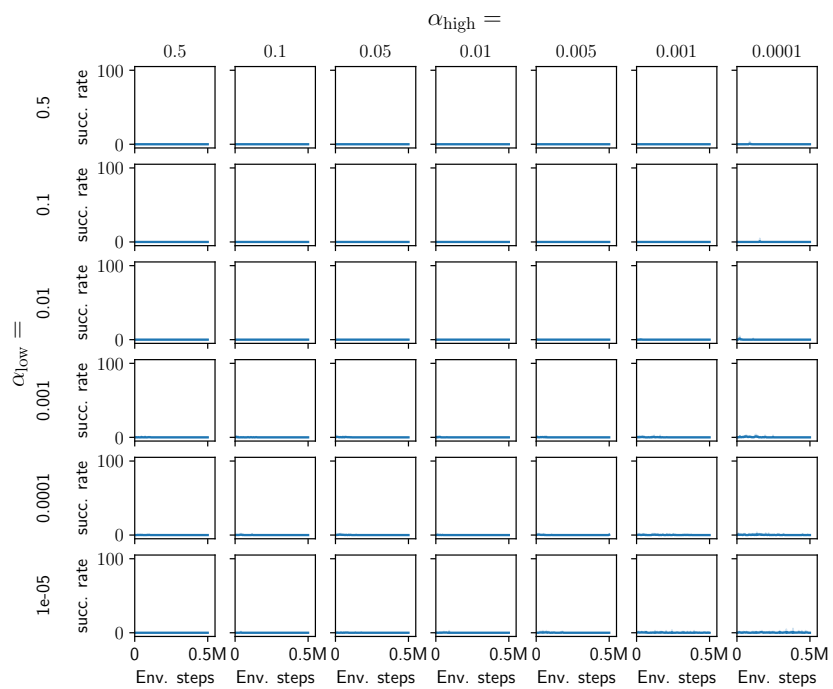


Figure S.26: Test performance of HAC agents on the LightsOutCursor environment for varying values for RelaxedBernoulli temperature τ and entropy targets $\alpha_{\text{high}}, \alpha_{\text{low}}$. We evaluate 5 individual agents per configuration. The best configuration is marked in **bold** ($\tau = 0.1, \alpha_{\text{low}} = 0.1, \alpha_{\text{high}} = 0.001$).

HAC, TileSwapCursor, temp 0.01



HAC, TileSwapCursor, temp 0.05



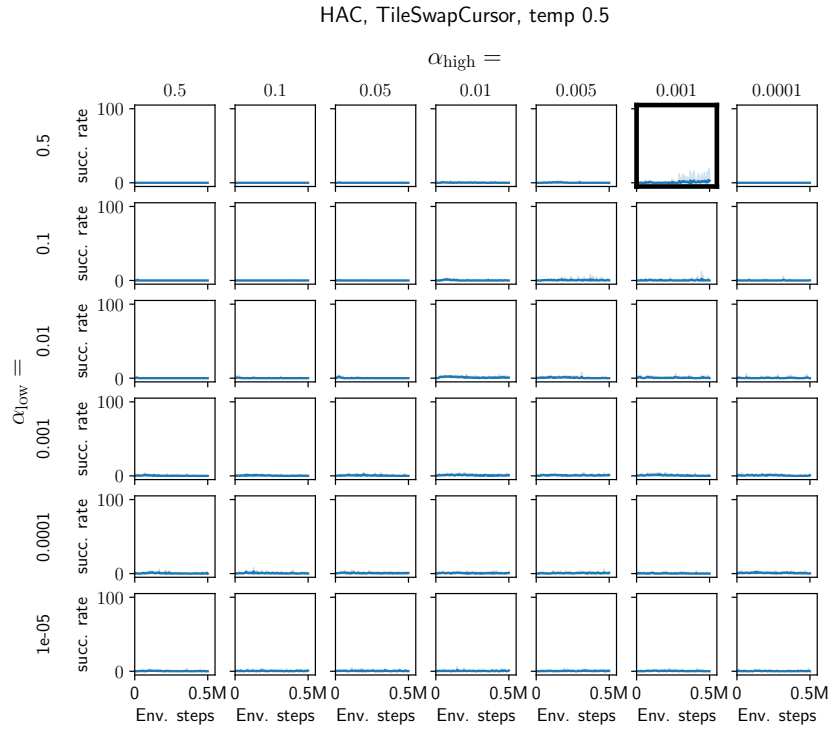
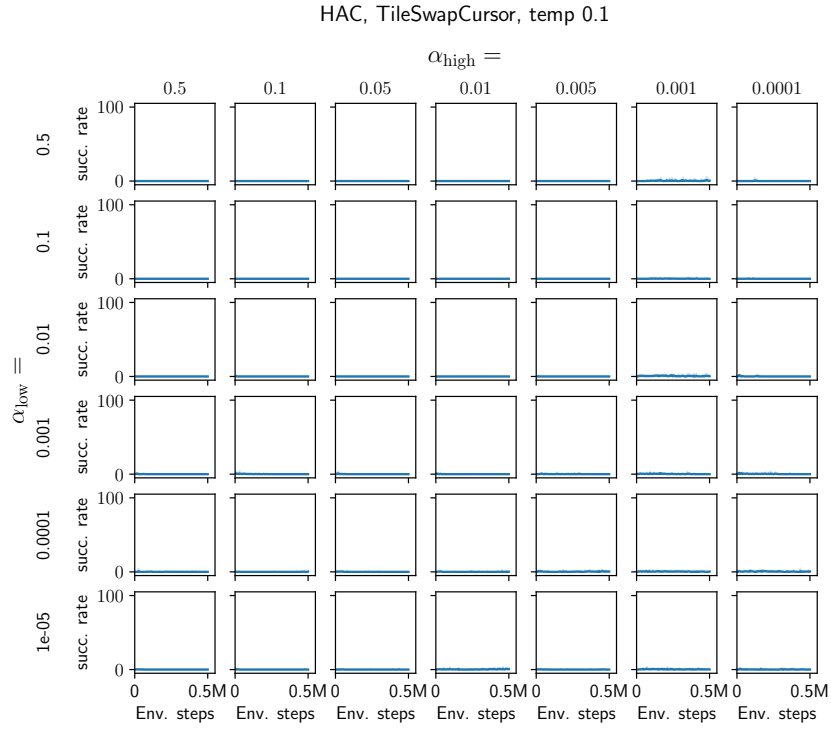


Figure S.26: Test performance of HAC agents on the TileSwapCursor environment for varying values for RelaxedBernoulli temperature τ and entropy targets $\alpha_{\text{high}}, \alpha_{\text{low}}$. We evaluate 5 individual agents per configuration. The best configuration is marked in **bold** ($\tau = 0.5, \alpha_{\text{low}} = 0.5, \alpha_{\text{high}} = 0.001$).

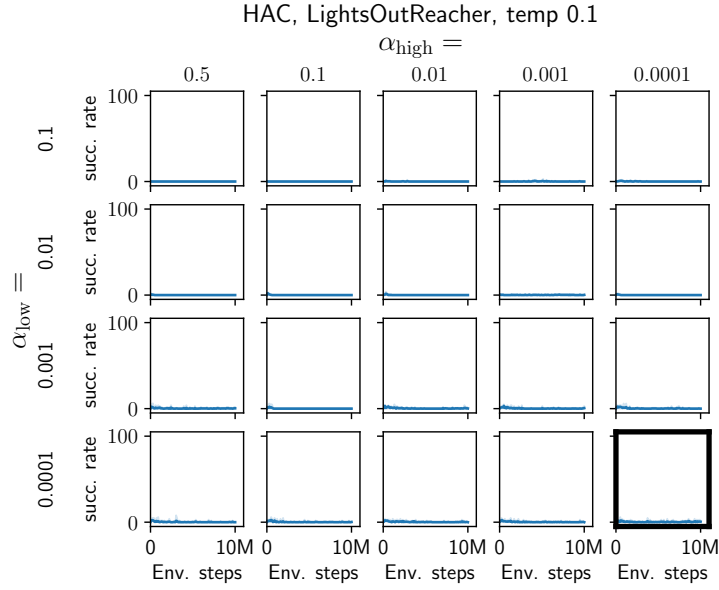


Figure S.27: Test performance of HAC agents on the LightsOutReacher environment for varying values for the entropy targets α_{high} , α_{low} and fixed RelaxedBernoulli temperature $\tau = 0.1$. We evaluate 5 individual agents per configuration. The best configuration is marked in **bold** ($\tau = 0.1$, $\alpha_{\text{low}} = 0.0001$, $\alpha_{\text{high}} = 0.0001$).

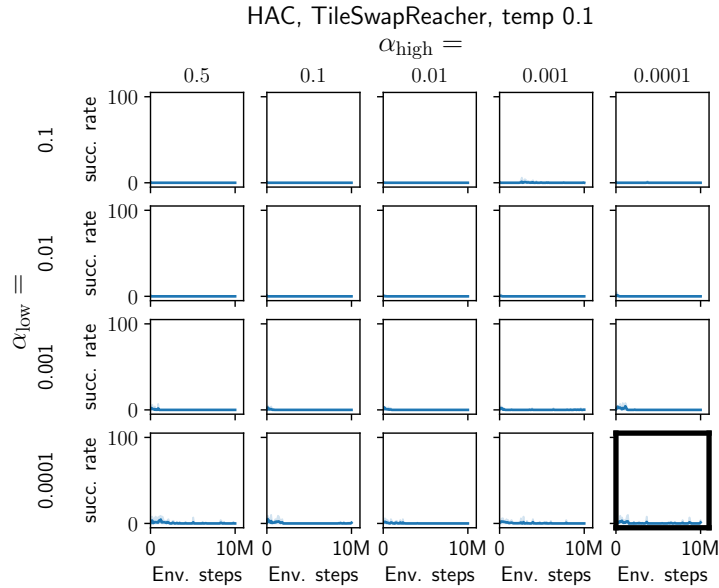


Figure S.28: Test performance of HAC agents on the TileSwapReacher environment for varying values for the entropy targets α_{high} , α_{low} and fixed RelaxedBernoulli temperature $\tau = 0.1$. We evaluate 5 individual agents per configuration. The best configuration is marked in **bold** ($\tau = 0.1$, $\alpha_{\text{low}} = 0.0001$, $\alpha_{\text{high}} = 0.0001$).

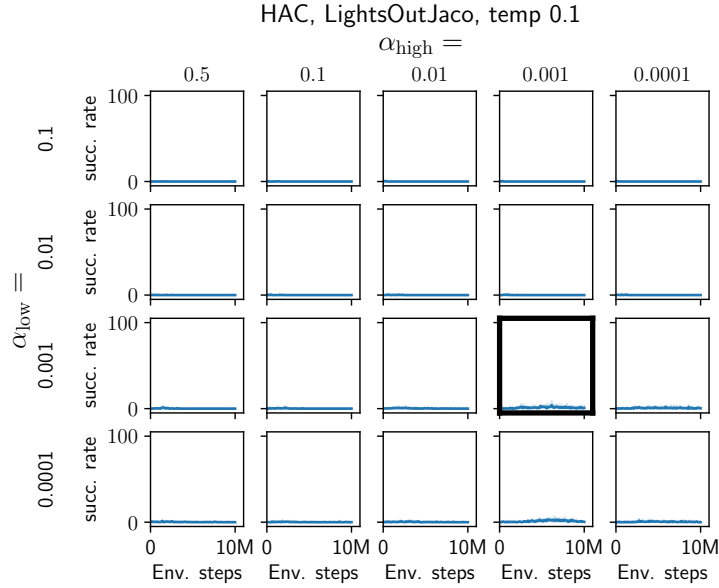


Figure S.29: Test performance of HAC agents on the LightsOutJaco environment for varying values for the entropy targets $\alpha_{\text{high}}, \alpha_{\text{low}}$ and fixed RelaxedBernoulli temperature $\tau = 0.1$. We evaluate 5 individual agents per configuration. The best configuration is marked in **bold** ($\tau = 0.1, \alpha_{\text{low}} = 0.001, \alpha_{\text{high}} = 0.001$).

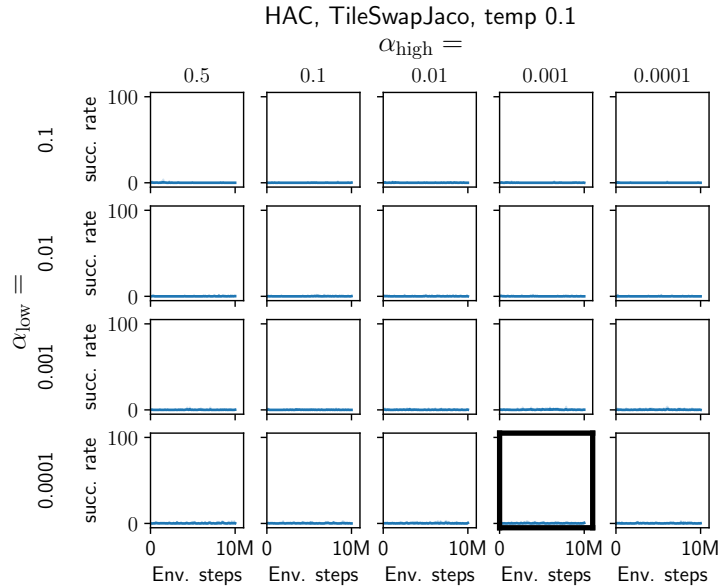


Figure S.30: Test performance of HAC agents on the TileSwapJaco environment for varying values for the entropy targets $\alpha_{\text{high}}, \alpha_{\text{low}}$ and fixed RelaxedBernoulli temperature $\tau = 0.1$. We evaluate 5 individual agents per configuration. The best configuration is marked in **bold** ($\tau = 0.1, \alpha_{\text{low}} = 0.0001, \alpha_{\text{high}} = 0.001$).

References

- [1] K. Gregor, D. J. Rezende, and D. Wierstra. “Variational Intrinsic Control”. In: *International Conference on Learning Representations (ICLR), Workshop Track Proceedings*. 2017. URL: <https://openreview.net/forum?id=Skc-Fo4Yg>.
- [2] uArm-Developer. *uArm-Python-SDK*. <https://github.com/uArm-Developer/uArm-Python-SDK>. 2021.
- [3] G. Brockman, V. Cheung, L. Pettersson, J. Schneider, J. Schulman, J. Tang, and W. Zaremba. “OpenAI Gym”. In: *CoRR* abs/1606.01540 (2016). arXiv: 1606.01540. URL: <http://arxiv.org/abs/1606.01540>.
- [4] H. B. Mann and D. R. Whitney. “On a Test of Whether one of Two Random Variables is Stochastically Larger than the Other”. In: *The Annals of Mathematical Statistics* 18.1 (1947), pp. 50–60. ISSN: 00034851. URL: <http://www.jstor.org/stable/2236101> (visited on 11/15/2022).
- [5] T. Haarnoja, A. Zhou, P. Abbeel, and S. Levine. “Soft Actor-Critic: Off-Policy Maximum Entropy Deep Reinforcement Learning with a Stochastic Actor”. In: *Proceedings of the 35th International Conference on Machine Learning (ICML)*. Vol. 80. Proceedings of Machine Learning Research. PMLR, 2018, pp. 1856–1865. URL: <http://proceedings.mlr.press/v80/haarnoja18b.html>.
- [6] D. P. Kingma and J. Ba. “Adam: A Method for Stochastic Optimization”. In: *3rd International Conference on Learning Representations, ICLR 2015, San Diego, CA, USA, May 7-9, 2015, Conference Track Proceedings*. 2015. URL: <http://arxiv.org/abs/1412.6980>.
- [7] P. Tandon. *pytorch-soft-actor-critic*. <https://github.com/pranz24/pytorch-soft-actor-critic>. 2021.
- [8] A. Levy. *Hierarchical-Actor-Critic-HAC*. <https://github.com/andrew-j-levy/Hierarchical-Actor-Critic-HAC>. 2020.
- [9] C. J. Maddison, A. Mnih, and Y. W. Teh. “The Concrete Distribution: A Continuous Relaxation of Discrete Random Variables”. In: *5th International Conference on Learning Representations (ICLR)*. 2017. URL: <https://openreview.net/forum?id=S1jE5L5gl>.
- [10] E. Jang, S. Gu, and B. Poole. “Categorical Reparameterization with Gumbel-Softmax”. In: *5th International Conference on Learning Representations (ICLR)*. 2017. URL: <https://openreview.net/forum?id=rkE3y85ee>.